This is to certify that the

thesis entitled

Remote sensing By Acoustic Video Pulse Techniques

presented by

Nai - Hsien Wang

has been accepted towards fulfillment
of the requirements for

Master degree in Electrical Engineering

Major professor

Date 2/18/88

REMOTE SENSING BY ACOUSTIC VIDEO PULSE TECHNIQUES

By

Nai-Hsien Wang

A THESIS

Submitted to

Michigan State University

in partial fulfillment of the requirements

for the degree of

MASTER OF SCIENCE

Department of Electrical Engineering and Systems Science

1988

ABSTRACT

REMOTE SENSING BY ACOUSTIC VIDEO PULSE TECHNIQUES

By

Nai-Hsien Wang

This thesis derives the formulas for acoustic wave equations in terms of an attenuation constant and the phase constant in material. The transmission coefficient and the reflection coefficient are found to be functions of (frequency) in dispersive media. According to the analytical results, the waveforms of the transmitted signal and the reflected signal depend not only on the characteristics of the medium, but also the frequency components of the incident signal. One can identify the different media by the reflected video pulse shapes and their spectral distributions. Experiments were designed and performed to show the validity of the theory.

Acknowledgements

I would like to express my sincere appreciation to Dr. Bong Ho and Dr. H. Roland Zapp, my advisors, for their guidance and support. I want to thank Mr. Di Ye for his help in the experiments. Most importantly, I would like to thank my parents, Mrs. and Mr. Chiou-Yueh and Chin-Chi Wang. Because of their encouragement and support, I was able to write this thesis.

Table of Contents

List of Tables

List of Figures

CHAPTER 1

Introduction

Most ultrasonic imaging systems use echo returns from boundaries of different acoustic impedances to show material properities. The image shows properties related to boundary variations. It is the purpose of the research reported here to show that the material characteristics can be extracted from the shape of the echo pulse when a narrow video pulse excitation is used. Although the video pulse technique has been used for a variety of applications in target identification by electromagnetic waves, it has not been applied to acoustic probing in spite of the advantage of lower operation frequencies and lower wave attenuation, since the attenuation coefficient is directly related to frequency. In addition to the lower operating frequency, another attractive feature is that the velocity of an acoustic wave (about 1500 m/sec in water) is five orders of magnitude lower than that of the electromagnetic wave in free space. Based on the relationship between frequency and wavelength for any propagating wave, $u = f\lambda$, the acoustic wave should have much shorter wavelength which in turn provides superior range resolution.

The video pulse radar signal contains a broadband of frequencies. For example, a signal that is approximately Gaussian in shape, as shown in Fig.

1.1.1, can be to expressed through its Fourier Transform as a spectrum of frequencies from about DC to 400 KHz. Each frequency component propagates through the material with a different velocity and attenuation depending upon the target and material properties. When all the reflected frequency components are received by the receiving antenna (transducer), the output will be a video pulse which resembles a spread version of the transmitted pulse. The reflection of each of the spectral components is determined by the characteristics of the medium from which it is reflected. This is due to the fact that the reflected pulse must satisfy the boundary conditions at each interface. For electromagnetic wave propagation, the dominant characteristics of the medium are the conductivity and the dielectric constant. For ultrasonic waves, the propagation and reflection depend on the medium density, elasticity, and viscosity.

Theoretically, the characteristics of a medium can be determined if the reflected and incident pulses are known. Conversely, if the incident pulse and the characteristics of the medium are known, it is possible to calculate the reflected pulse shape. By using a Gaussian video pulse in the time domain as the incident pulse, and by taking typical values of density, elasticity, and viscosity of media, it is possible to calculate the reflected pulse from materials such as soil, wood, stone and metal (Figure 1.1.3). The calculated pulse shapes show that the reflected pulses are different for different

media.

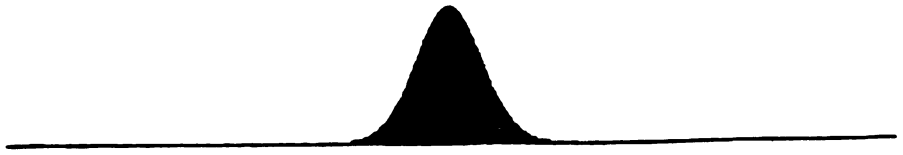

Figure 1.1.1 A Gaussian video pulse

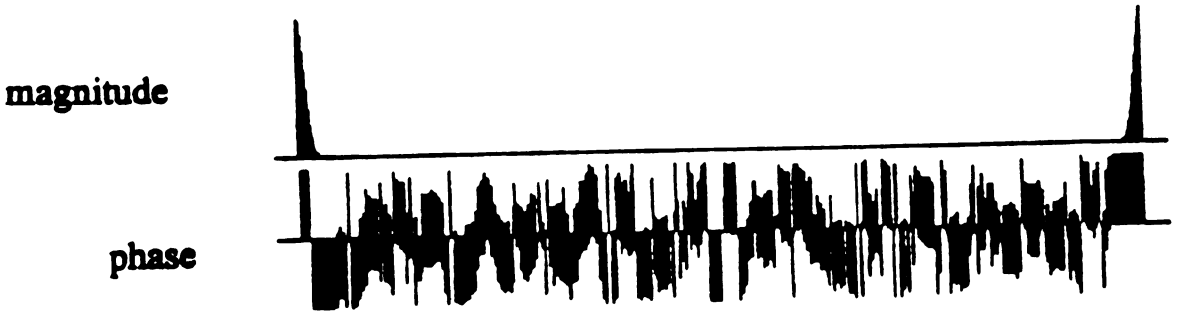

Figure 1.1.2 The spectrum of a Gaussian video pulse

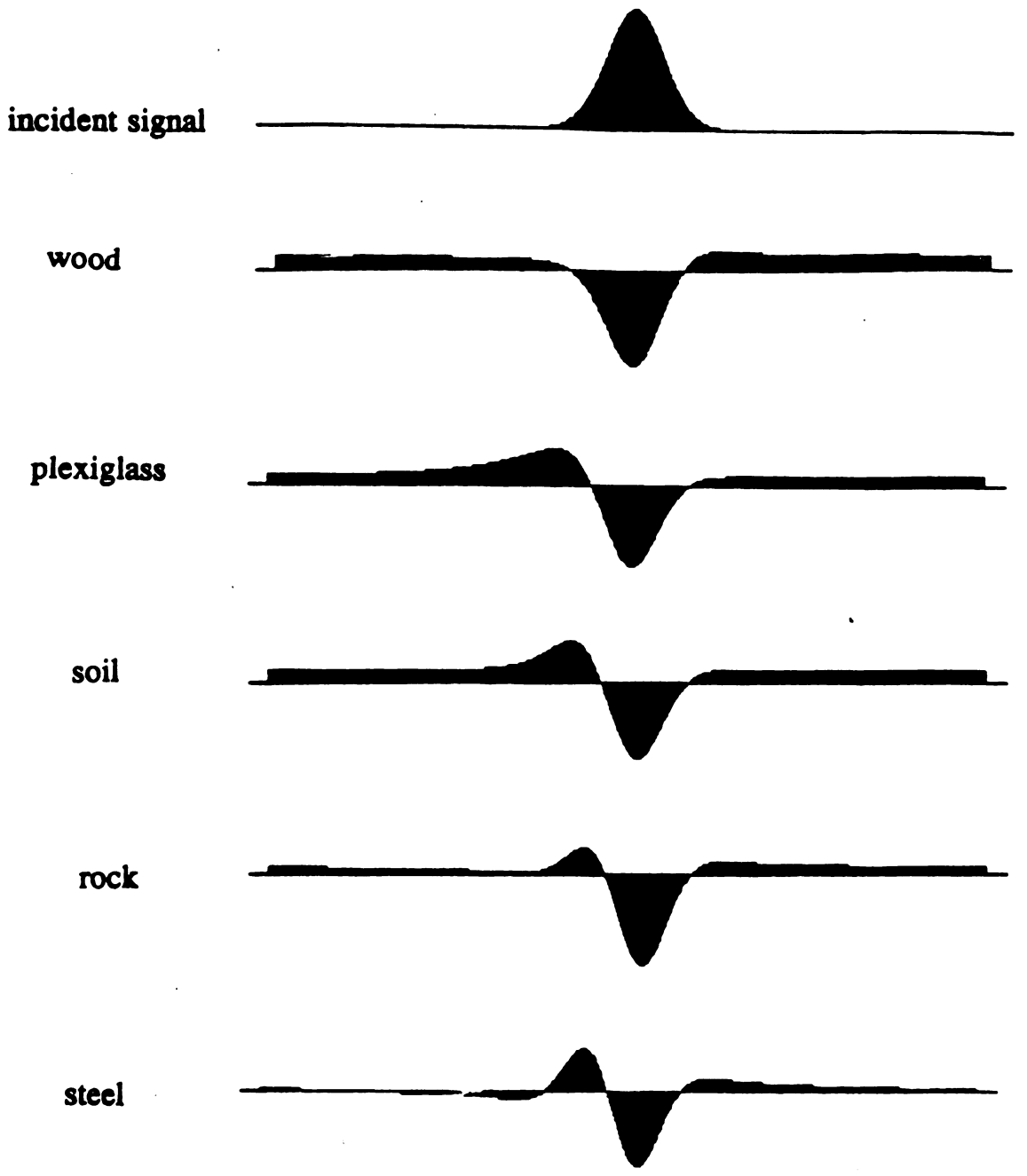

Figure 1.1.3 The reflected signals from some materials

CHAPTER 2

Theoretical Considerations

This chapter provides the theoretical analysis for the acoustic video pulse probing techniques. In the first section, some related ultrasound principles are reviewed. The acoustic plane wave equation is derived in the second section. In the third section, the transmission coefficient and the reflection coefficient are determined from the boundary conditions at interfaces. In reality, ultrasound propagating through a medium will have some energy loss, so the damping and attenuation properties should also be taken into consideration. This problem will be discussed in section 2.4. The properties of the acoustic video pulse will be explained in section 2.5. Since the acoustic wave is very similar to the electromagnetic wave, the commonelity will be formulated in section 2.6.

2.1 Review of Basic Ultrasound Principles

Ultrasound is the name given to those waves with frequencies above 20 KHz (above the audible range). Ultrasonic waves consist of propagating periodic disturbances in an elastic medium. The particles of the medium vibrate about their equilibrium positions either perpendicular to or parallel to the direction of propagation. Since the parallel vibrations are dominant and

of lower propagation losses only these variations will be considered. The propagation of the resulting motion-strain effects away from the source results in a longitudinal compression wave that transmits mechanical, or acoustic, energy away from the source. The vibratory motion of the medium is strongly dependent on the ultrasound frequency and on the state of the medium. Table 2.1.1 provides that the values of velocity of longitudinal sound waves in various materials. Velocity in solids are the highest, those in liquids and biological soft tissues are lower, and those in gases are lowest.

The relationship between frequency and wavelength of a wave is given by

$$\lambda = \frac{u}{f} \tag{2.1.1}$$

where u is the propagation velocity, f the the frequency of the wave, and λ is the wavelength. Since the propagation velocity of ultrasound (1.5×10^3 *m/sec* in water) is much lower than that of an electromagnetic wave (3×10^8 *m/sec* in free space), the wavelength of ultrasound is five orders of magnitude smaller for a given frequency. For a frequency of 5 MHz, the wavelength of ultrasound is approximately 0.3 mm while for an electromagnetic wave it is 60 meters. Because of the much shorter wavelength, the use of ultrasound for detection will give much higher resolution.

Table 2.1.1 Approximate values of ultrasonic velocities of various media [1]

Medium	Sound Velocity (m/sec)
Dry air (20^0C)	343.6
Water (37^0C)	1524
Amniotic fluid	1530
Brain	1525
Fat	1485
Liver	1570
Muscle	1590
Tendon	1750
Skull bone	3360
Uterus	1625

2.2 The acoustic plane wave equation

In this section, we will investigate sound propagation in an infinite homogeneous medium in equilibrium. The coordinate system is shown in Figure 2.2.1. If a force is applied in the x-direction, it will result in a uniform pressure $p(x_0,t)$ to the y-z plane at a distance x_0 from the origin. Due

to this applied force, the particles will experience a displacement in the x-direction. Particles at the location x_0 will also be displaced. If we consider a small differential volume element with incremental length dx and area A in the plane of the applied force, the equilibrium volume, V, of the element will be

$$V = A\,dx \tag{2.2.1}$$

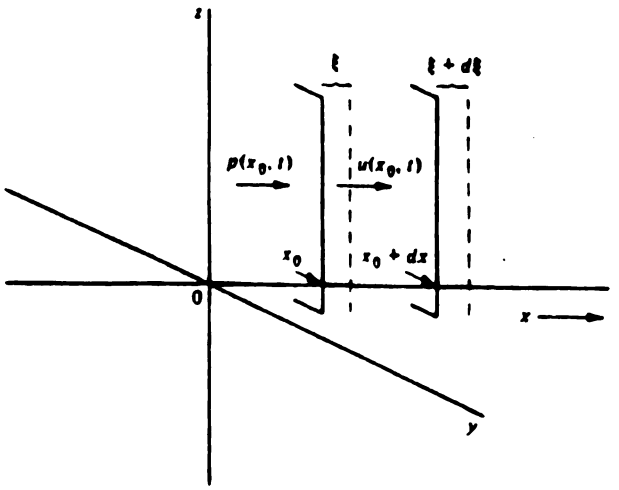

Figure 2.2.1 Infinite homogeneous medium with plane applied pressure

As a result of this compressional force the differential volume changes to

$$V' = A\,(dx+d\xi) = A\,(dx + \frac{\partial \xi}{\partial x}\,dx) \tag{2.2.2}$$

where $d\xi$ represents a compressional displacement.

Therefore, the change in volume is

$$dV = V' - V = A\,(\frac{\partial \xi}{\partial x}\,dx) \tag{2.2.3}$$

Conventionally, the strain produced in the volume element is defined as the ratio of the volume change to the original volume:

$$strain \equiv \frac{dV}{V} = \frac{\partial \xi}{\partial x} \tag{2.2.4}$$

According to Hooke's law, the ratio of stress to strain in an elastic medium is constant. This relationship can be expressed as

$$p = -k\frac{\partial \xi}{\partial x} \tag{2.2.5}$$

where k is the coefficient of elasticity. The negative sign in Eq.(2.2.5) results from a positive pressure in the x-direction giving a strain in the negative x-direction.

We can define the particle velocity u as the time rate of change of particle displacement. That is,

$$u(x,t) = \frac{\partial \xi}{\partial t} \tag{2.2.6}$$

The partial derivative of Eq.(2.2.5), with respect to time, gives:

$$\frac{\partial p}{\partial t} = -k\frac{\partial}{\partial t}\left(\frac{\partial \xi}{\partial x}\right) = -k\frac{\partial u}{\partial x} \tag{2.2.7}$$

or

$$\frac{\partial u}{\partial x} = \frac{-1}{k}\frac{\partial p}{\partial t} \tag{2.2.8}$$

If the applied pressure varies with time, the pressure magnitude will be a function of distance, x, as well as of time, t. From Newton's second law of motion, the acceleration of a material element resulting from an applied

pressure is:

$$\frac{\partial p}{\partial x} = -\rho \frac{\partial u}{\partial t} \tag{2.2.9}$$

The negative sign in Eq. (2.2.9) results from a net acceleration to the right for a negative spatial pressure gradient. In Eq. (2.2.9) ρ is the medium density.

Eq.(2.2.8) and Eq.(2.2.9) are the coupled equations relating to pressure particle velocity. By decoupling these equations, it is possible to obtain the acoustic plane wave equations

$$\frac{\partial^2 p}{\partial t^2} = \frac{k}{\rho} \frac{\partial^2 p}{\partial x^2} \tag{2.2.10}$$

and,

$$\frac{\partial^2 u}{\partial t^2} = \frac{k}{\rho} \frac{\partial^2 u}{\partial x^2} \tag{2.2.11}$$

The general solution for pressure and particle velocity are

$$p = p(0)e^{j(\omega t - Kx)} \tag{2.2.12}$$

$$u = u(0)e^{j(\omega t - Kx)} \tag{2.2.13}$$

where K is the wave propagation constant given by

$$K = \omega\sqrt{\rho/k} \triangleq \frac{\omega}{c} \qquad c = \sqrt{\frac{k}{\rho}} \tag{2.2.14}$$

The wave number K is in general a complex quantity. It consists of the phase constant β and the attenuation constant α,

$$K = \beta - j\alpha \tag{2.2.15}$$

From Eq.(2.2.12), Eq.(2.2.13) and Eq. (2.2.9), the relationship between pressure and particle velocity is

$$p = \frac{\omega\rho}{K}u \tag{2.2.16}$$

The characteristic acoustic impedance is defined as the ratio of the pressure to particle speed. From Eq.(2.2.15), the acoustic impedance Z can be expressed as

$$Z \equiv \frac{p}{u} = \frac{\omega\rho}{K} \tag{2.2.17}$$

For a lossy medium, the acoustic impedance is a complex quantity. For a lossless medium the attenuation constant α is zero, and the wave number reduces to $K = \beta$, which gives a real acoustic impedance.

Under the lossless assumption, the phase velocity v_p is

$$v_p = \frac{\omega}{\beta} = \frac{\omega}{K} \tag{2.2.18}$$

Therefore, the acoustic impedance for a lossless medium can be written as

$$Z = \rho v_p \tag{2.2.19}$$

For an attenuation constant of zero, the mass density, the longitudinal wave velocity and the acoustic impedance of some materials are shown in Table 2.2.1.

Table 2.2.1 Characteristics of some materials [6]

Material	Mass Density kg/m^3	Longitudinal Velocity, m/s	Acoustic Impedance $\times 10^6\ kg/m^2 \cdot s$
Air (20^0C)	1.21	340	411×10^{-6}
Water (20^0C)	1,000	1,480	1.5
Aluminum	2,695	6,350	17.1
Plexiglass	1,182	2,680	3.17
Silicon rubber	1,010	1,030	1.04
Lead	11,400	1,960	22.3
Copper	8,900	4,700	42
Iron (steel)	7,830	5,950	46.6

2.3 Transmission and reflection coefficients

When an acoustic plane wave is incident to a boundary between two different media, it will be partially reflected. The ratio of the characteristic impedances of the two media determines the magnitude of the reflection coefficient and transmission coefficient. Assume there is an acoustic plane wave propagating from medium 1 to medium 2, as shown in Figure 2.3.1. Snell's law states that the angles of incidence and reflection are equal when the wavelength of the wave is small compared to the dimensions of the

reflector. That is,

$$\theta_i = \theta_r \tag{2.3.1}$$

From relationship between θ_i and θ_t, the angle of transmission, is:

$$\frac{\sin\theta_i}{\sin\theta_t} = \frac{u_1}{u_2} \tag{2.3.2}$$

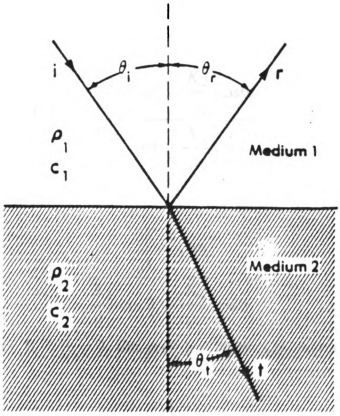

Figure 2.3.1 Transmission and reflection at an interface

In the equilibrium state, the pressure on both sides of the boundary remains the same in order to maintain a stationary boundary. This gives

$$p_i + p_r = p_t \tag{2.3.3}$$

Furthermore, the normal component of the particle velocity must be the

same on both sides of the boundary or else the two media will not remain in contact. Thus,

$$u_i\cos\theta_i - u_r\cos\theta_r = u_t\cos\theta_t \tag{2.3.4}$$

From Eqs.(2.2.16) and (2.3.4), we have

$$\frac{p_i K_1 \cos\theta_i}{\rho_1} - \frac{p_r K_1 \cos\theta_r}{\rho_1} = \frac{p_t K_2 \cos\theta_t}{\rho_2} \tag{2.3.5}$$

Solving Eqs.(2.3.3) and (2.3.5), the pressure ratios are

$$\frac{p_r}{p_i} = \frac{\frac{K_1}{\rho_1}\cos\theta_i - \frac{K_2}{\rho_2}\cos\theta_t}{\frac{K_1}{\rho_1}\cos\theta_i + \frac{K_2}{\rho_2}\cos\theta_t} \tag{2.3.6}$$

and

$$\frac{p_t}{p_i} = \frac{\frac{2K_1}{\rho_1}\cos\theta_i}{\frac{K_1}{\rho_1}\cos\theta_i + \frac{K_2}{\rho_2}\cos\theta_t} \tag{2.3.7}$$

For normal incidence $\theta_i = \theta_t = 0$, the pressure amplitude ratios are reduced to

$$\textit{Reflection coefficient } R = \frac{p_r}{p_i} = \frac{\frac{K_1}{\rho_1} - \frac{K_2}{\rho_2}}{\frac{K_1}{\rho_1} + \frac{K_2}{\rho_2}} \tag{2.3.8}$$

$$\textit{Transmission coefficient } T = \frac{p_t}{p_i} = \frac{\frac{2K_1}{\rho_1}}{\frac{K_1}{\rho_1} + \frac{K_2}{\rho_2}} \tag{2.3.9}$$

Using the acoustic impedance definition $Z = \omega\rho/K$, the reflection coefficient and transmission coefficient can be reduced to:

$$R = \frac{Z_2 - Z_1}{Z_2 + Z_1} \qquad (2.3.10)$$

$$T = \frac{2Z_2}{Z_2 + Z_1} \qquad (2.3.11)$$

Up to this point, the reflection and transmission coefficients were expressed in the time domain. Using the Fourier Transform the reflection and transmission coefficients can be expressed in the frequency domain as well.

The Fourier Transform of $p(x,t)$ is defined as

$$P(x,\omega) = \int_{-\infty}^{\infty} p(x,t)e^{-j\omega t}dt \qquad (2.3.12)$$

Because the reflection coefficient R and the transmission coefficient T are independent of time, the R and T can be written as

$$R = \frac{P_r(0,\omega)}{P_i(0,\omega)} = \frac{\frac{K_1}{\rho_1} - \frac{K_2}{\rho_2}}{\frac{K_1}{\rho_1} + \frac{K_2}{\rho_2}} = \frac{Z_2 - Z_1}{Z_2 + Z_1} \qquad (2.3.13)$$

$$T = \frac{P_t(0,\omega)}{P_i(0,\omega)} = \frac{\frac{2K_1}{\rho_1}}{\frac{K_1}{\rho_1} + \frac{K_2}{\rho_2}} = \frac{2Z_2}{Z_2 + Z_1} \qquad (2.3.14)$$

2.4 Damping and attenuation

As discussed in section 2.2, the acoustic wave equation (Eqs.(2.2.10) and (2.2.11)) was derived for the condition that the wave propagating through the medium suffers no energy loss, that is, the acoustic wave propagates in the medium without attenuation. Ideal materials of this kind do not exist, although weakly damped materials are often approximated as ideal. Elastic damping usually depends on temperature, frequency, and the type of vibration. At room temperature, acoustic losses in many materials may be adequately described by either assuming the (1) elasticity k is a complex quantity or by (2) adding a viscous damping term.

In the following section, both of these approaches are used to obtain the attenuation constant α and phase constant β. The results from these approaches are then compared and discussed.

2.4.1 Complex elasticity

In a lossy medium the elasticity k becomes a complex number, that is,

$$k = k_r + jk_i \tag{2.4.1}$$

From Eq.(2.2.14), the wave number K becomes

$$K = \omega\sqrt{\rho/(k_r + jk_i)} \tag{2.4.2}$$

and jK contains real and imaginary parts:

$$jK = \alpha + j\beta \tag{2.4.3}$$

If we insert Eq.(2.4.3) into Eq.(2.4.2) and equate the real and imaginary parts the following relationships result:

$$\beta^2 - \alpha^2 = \frac{\omega^2 \rho k_r}{k_r^2 + k_r^2} \tag{2.4.4}$$

$$2\alpha\beta = \frac{\omega^2 \rho k_i}{k_r^2 + k_r^2} \tag{2.4.5}$$

Using these equations, the attenuation constant α and the phase constant β can be expressed in terms of ω, ρ, k_r and k_i:

$$\alpha = \omega\sqrt{\rho k_r/2}\ \left[\frac{\sqrt{1+(k_i/k_r)^2}-1}{k_r^2+k_i^2}\right]^{1/2} \tag{2.4.6}$$

$$\beta = \omega\sqrt{\rho k_r/2}\ \left[\frac{\sqrt{1+(k_i/k_r)^2}+1}{k_r^2+k_i^2}\right]^{1/2} \tag{2.4.7}$$

or, alternatively k_i and k_r in terms of α and β as:

$$k_r = \frac{\omega^2\rho(\beta^2-\alpha^2)}{(\beta^2+\alpha^2)^2} \tag{2.4.8}$$

$$k_i = \frac{2\omega^2\rho\alpha\beta}{(\beta^2+\alpha^2)^2} \tag{2.4.9}$$

In the case of a low loss medium, that is when $(\frac{k_i}{k_r})^2 << 1$, the α and β reduce to

$$\alpha \approx \frac{\omega}{2}(\frac{k_i}{k_r})\sqrt{\rho/k_r} \tag{2.4.10}$$

$\sqrt{1+(\frac{k_i}{k_r})^2} \approx 1+\frac{1}{2}(\frac{k_i}{k_r})^2$

$\therefore \alpha = \frac{\omega}{2}\sqrt{\rho k_r}\ \frac{1}{k_r}\left[\frac{(\frac{k_i}{k_r})^2}{1+(\frac{k_i}{k_r})^2}\right]^{\frac{1}{2}}$

$= \frac{\omega}{2}\sqrt{\frac{\rho}{k_r}}(\frac{k_i}{k_r})$

$$\beta \approx \omega\sqrt{\rho/k_r}\ \left[\frac{1+\frac{1}{4}\left(\frac{k_i}{k_r}\right)^2}{1+\left(\frac{k_i}{k_r}\right)^2}\right]^{1/2}$$

$$\approx \omega\sqrt{\rho/k_r}\ \left[1-\frac{3}{8}\left(\frac{k_i}{k_r}\right)^2\right] \qquad (2.4.11)$$

2.4.2 Damping force

The second approach to obtaining the attenuation and phase constants is to consider the damping force term in the wave equation. In an ideal loss-less medium, Hooke's law describes the linear relationship between pressure and strain:

$$p_{ideal} = -c\,S \qquad (2.4.12)$$

where c is a proportional constant, called elastic stiffness constant, while S is strain, as defined in Eq.(2.2.4).

The damping force in material can be put in the form:

$$p_{damping} = -\eta\frac{\partial S}{\partial t} \qquad (2.4.13)$$

where η is the material viscosity.

The total pressure becomes

$$p = p_{ideal} + p_{damping} = -\left(kS + \eta\frac{\partial S}{\partial t}\right) \qquad (2.4.14)$$

For a one-dimensional problem, the strain is

$$S = \frac{\partial \xi}{\partial x} \qquad (2.4.15)$$

From Eqs.(2.2.6) and (2.4.15) we get

$$\frac{\partial u}{\partial x} = \frac{\partial^2 \xi}{\partial x \partial t} = \frac{\partial S}{\partial t} \tag{2.4.16}$$

Taking a partial derivative with respect to time in Eq.(2.4.14), we obtain:

$$\frac{\partial p}{\partial t} = -c\frac{\partial u}{\partial x} - \eta \frac{\partial^2 u}{\partial x \partial t} \tag{2.4.17}$$

From Newton's second low of motion, Eq.(2.2.9), the spatial derivative of pressure and the time derivative of particle velocity are related by

$$\frac{\partial p}{\partial x} = -\rho \frac{\partial u}{\partial t} \tag{2.4.18}$$

Following the same procedure used in section 2.2 to decouple Eqs.(2.4.17) and (2.4.18), the acoustic plane wave equations including attenuation becomes:

$$\frac{\partial^2 p}{\partial t^2} = \frac{c}{\rho}\frac{\partial^2 p}{\partial x^2} + \frac{\eta}{\rho}\frac{\partial^3 p}{\partial x^2 \partial t} \tag{2.4.19}$$

and,

$$\frac{\partial^2 u}{\partial t^2} = \frac{c}{\rho}\frac{\partial^2 u}{\partial x^2} + \frac{\eta}{\rho}\frac{\partial^3 u}{\partial x^2 \partial t} \tag{2.4.20}$$

Again, the general solutions for pressure and velocity are

$$p = p(0)e^{j(\omega t - Kx)} \tag{2.4.21}$$

$$u = u(0)e^{j(\omega t - Kx)} \tag{2.4.22}$$

where

$$K = \beta - j\alpha \tag{2.4.23}$$

Using these solutions, the following equations are obtained:

$$\rho\omega^2 p = cK^2 p + j\eta K^2 \omega p \tag{2.4.24}$$

$$\rho\omega^2 = cK^2 + j\eta K^2 \omega \tag{2.4.25}$$

With $K^2 = \beta^2 - 2\alpha\beta j - \alpha^2$, and both α and β real, the following equations are obtained by equating the real and imaginary parts of Eq. (2.4.25).

$$c(\beta^2 - \alpha^2) + 2\alpha\beta\eta\omega = \rho\omega^2 \tag{2.4.26}$$

$$\eta\omega(\beta^2 - \alpha^2) - 2\alpha\beta c = 0 \tag{2.4.27}$$

Solving Eqs. (2.4.26) and (2.4.27) for real α and β, gives:

$$\alpha^2 = \frac{1}{2}\frac{c\rho\omega^2}{(\eta^2\omega^2 + c^2)}[\sqrt{1 + (\eta\omega/c)^2} - 1] \tag{2.4.28}$$

and

$$\beta^2 = \frac{1}{2}\frac{c\rho\omega^2}{(\eta^2\omega^2 + c^2)}[\sqrt{1 + (\eta\omega/c)^2} + 1] \tag{2.4.29}$$

Finally,

$$\alpha = \omega\left\{\frac{1}{2}\frac{c\rho}{(\eta^2\omega^2 + c^2)}[\sqrt{1 + (\eta\omega/c)^2} - 1]\right\}^{1/2} \tag{2.4.30}$$

$$\beta = \omega\left\{\frac{1}{2}\frac{c\rho}{(\eta^2\omega^2 + c^2)}[\sqrt{1 + (\eta\omega/c)^2} + 1]\right\}^{1/2} \tag{2.4.31}$$

The above equations give the general solution for the attenuation constant α and phase constant β. We can express c and η in terms of α and β as:

$$c = \frac{\rho\omega^2(\beta^2 - \alpha^2)}{(\beta^2 + \alpha^2)^2} \tag{2.4.32}$$

$$\eta\omega = \frac{2\rho\omega^2\alpha\beta}{(\beta^2+\alpha^2)^2} \tag{2.4.33}$$

or,

$$\eta = \frac{2\rho\omega\alpha\beta}{(\beta^2+\alpha^2)^2} \tag{2.4.34}$$

For the low frequency approximation $(\frac{\eta\omega}{c})^2 << 1$, the following simplifications result:

$$\alpha \approx \frac{\eta\omega^2}{2c}\sqrt{\rho/c}\,[1-(\eta\omega/c)^2]^{1/2}$$

$$\approx \frac{\eta\omega^2}{2c}\sqrt{\rho/c}\,[1-\frac{1}{2}(\frac{\eta\omega}{c})^2]^{1/2} \tag{2.4.35}$$

$$\approx \frac{\eta\omega^2}{2c}\sqrt{\rho/c} \tag{2.4.36}$$

$$\beta \approx \omega\sqrt{\rho/c}\,[1-\frac{3}{4}(\frac{\eta\omega}{c})^2]^{1/2}$$

$$\approx \omega\sqrt{\rho/c}\,[1-\frac{3}{8}(\frac{\eta\omega}{c})^2] \tag{2.4.37}$$

$$\approx \omega\sqrt{\rho/c} \tag{2.4.38}$$

From Eqs.(2.4.36) and (2.4.38), when the frequency of the acoustic wave is low ($\omega << (\frac{c}{\eta})$), the attenuation constant is proportion to ω^2, and the phase constant is proportion to ω. For very low frequencies, the attenuation approaches zero. For higher frequencies the attenuation increases rapidly.

For a given frequency, the attenuation constant α is proportion to the square root of the medium density. As the viscosity constant increases, the attenuation constant also increases. If the the elasticity stiffness constant

increased, the attenuation constant decreases.

By comparing the results of these two approaches, that is, using complex elasticity or using an added damping force, the same results conclusions can be drawn. From Eqs.(2.4.6), (2.4.7), (2.4.30) and (2.4.31), we found that the real part k_r of the complex elasticity plays the same role as the elasticity c in the lossless case. The imaginary part k_i of the complex elasticity is analogous to the damping constant η times angular frequency ω. That is,

$$k_r \longleftrightarrow c$$

$$k_i \longleftrightarrow \eta\omega$$

2.5 Video pulse probing techniques

Reflection coefficients and transmission coefficients are crucial factors in determining wave propagation in media with different materials properties. When the incident wave is a narrow band signal, the reflection coefficient and the transmission coefficient are usually constant. This is not true for a broad band signal. The basic principle of using video pulses is to exploit the broad band signal characteristics to detect media variations. The broadband signal form the transducer is dispersed by the frequency dependent reflection and transmission at the interfaces of different acoustic

impedances of different media. The energy of the reflected wave or of the transmitted wave depends on the frequency dependent reflection coefficient or the frequency dependent transmission coefficient.

A necessary requirement for using video pulses is that the waveform of the incident wave in both time and frequency must be well known. When the video pulse impings on the interface between the first and second media, the reflected wave contains all frequency components, each modified by its own frequency dependent reflection coefficient. The reflected signal spectrum contains the information necessary to characterize the unknown media.

The Fourier spectrum of the incident pressure wave is given by:

$$P_i(x,\omega) = \int_{-\infty}^{\infty} p_i(x,t)e^{-j\omega t}dt \qquad (2.5.1)$$

If x is set to zero at the interface of two media, the pressure in the frequency domain at the interface is:

$$P_i(0,\omega) = F<p(0,t)> \qquad (2.5.2)$$

where $F<\cdot> = \int_{-\infty}^{\infty} \cdot\, e^{-j\omega t}dt$ is the Fourier transformation.

In section 2.3, it was shown that the reflection coefficient is independent of time, so that the Fourier Transform of the reflected wave at the interface in the frequency domain is given by:

$$P_r(0,\omega) = P_i(0,\omega)R \tag{2.5.3}$$

and the reflected pressure wave at the interface in the time domain is

$$p_r(0,t) = F^{-1} <P_r(0,\omega)> = F^{-1}<P_i(0,\omega)\, R> \tag{2.5.4}$$

where $F^{-1}< \cdot > = \frac{1}{2\pi}\int_{-\infty}^{\infty} \cdot\, e^{j\omega t} d\omega$ is the inverse Fourier transform and R is the time independent reflection coefficient.

A detected signal a distance d from the interface has the form:

$$p_r(d,t) = p_r(0,t)e^{-jK_1 d} \tag{2.5.6}$$

The signal to be detected is thus given by:

$$p_r(x,t) = \mathrm{Re}\left\{ F^{-1}<P_i(0,\omega)R>e^{-jK_1 d} \right\} \tag{2.5.7}$$

$$= \mathrm{Re}\left\{ F^{-1}< F<p_i(0,t)> R > e^{-jK_1 d} \right\}$$

The real part of the pressure is taken since only this signal can be detected experimentally.

2.6 Analogy between ultrasonic waves and electromagnetic waves

The equations for the acoustic plane waves have many similarities to electromagnetic waves. As shown in Table 2.6.1, the pressure and particle velocity of the acoustic wave play the same role as the electrical field and

magnetic intensity of the electromagnetic wave. The magnitude of the pressure provides the potential energy and the particle velocity provides the kinetic energy. The density and the reciprocal of the elasticity are analogous to the permeability and permittivity, respectively.

Table 2.6.1 Analogy between ultrasonic waves and electromagnetic waves

Ultrasound	Electromagnetic wave
pressure p	electric field E
particle velocity u	magnetic intensity H
momentum density ρu	magnetic flux density $B = \mu H$
Strain $S = \dfrac{p}{elasticity\ k}$	electric flux density $D = \varepsilon E$
density ρ	permeability μ
$\dfrac{1}{elasticity\ k}$	permittivity ε
wave number $K = \omega\sqrt{\rho/k}$	wave number $K = \omega\sqrt{\mu\varepsilon}$
phase velocity $v = \dfrac{\omega}{\beta}$	phase velocity $v = \dfrac{\omega}{\beta}$
wave equation	wave equation
$\dfrac{\partial^2 p}{\partial x^2} = \dfrac{\rho}{k}\dfrac{\partial^2 p}{\partial t^2}$	$\dfrac{\partial^2 E}{\partial x^2} = \mu\varepsilon\dfrac{\partial^2 E}{\partial t^2}$
$\dfrac{\partial^2 u}{\partial x^2} = \dfrac{\rho}{k}\dfrac{\partial^2 u}{\partial t^2}$	$\dfrac{\partial^2 H}{\partial x^2} = \mu\varepsilon\dfrac{\partial^2 H}{\partial t^2}$

CHAPTER 3

Experimental Procedure

In order to analyze the characteristics of an unknow medium, we must detect and process the reflected or transmitted waveform. Although the transmitted waveform carries more information about the unknow medium, it is, more difficult to obtain because of the medium dimensions. Furthermore, the implementation of a transmission configuration requires two transducers while the reflection technique uses only one transducer. Thus the echo mode of operation is the choice of preference.

In order to demonstrate the theory developed, a single layer target is used for simplicity. The ultrasonic transceiver transducer is submerged in water. When the ultrasonic pulse hits the water/target interface it generates a reflected wave which travels back to the transducer. By comparing the reflected wave and the incident wave, the reflection coefficient of the interface can be determined. Two experimental procedures are performed, the reflected wave is recorded in real time and the recorded signal is processed through various signal processing techniques to retrieve information about the target. For accurate waveform recording, a high sampling analog-to-digital converter is required. According to the Nyquist criteria, the sampling frequency must be at least twice the highest frequency component of the

signal. The higher the sampling rate, the better the recorded signal. In the experiments reported here with a transducer frequency of 2.25 MHz a sampling rate of 14.667 MHz about 3.26 times of the Nyquist rate was chosen. Additional data processing of the recorded signal is performed by various algorithms.

In section 3.1 the experimental configurations are presented and in section 3.2 the data processing algorithms are discussed.

3.1 Experimental Configurations

In order to determine the properties of a medium, the characteristics of the incident signal and reflected signal waveforms must be known. The system shown in Figure 3.1.1 is used to obtain the signal from the water/target interface.

3.1.1 Sampling the incident signal waveform

The video pulse technique requires that a broadband signal, ideally an impulse, be transmitted for optimum material characterization. Experimentally, a pulse of less than 50μsec is transmitted.

For subsequent analysis, a detailed incident wave sent out by the transducer has to be known precisely. A simple way to obtain such a waveform

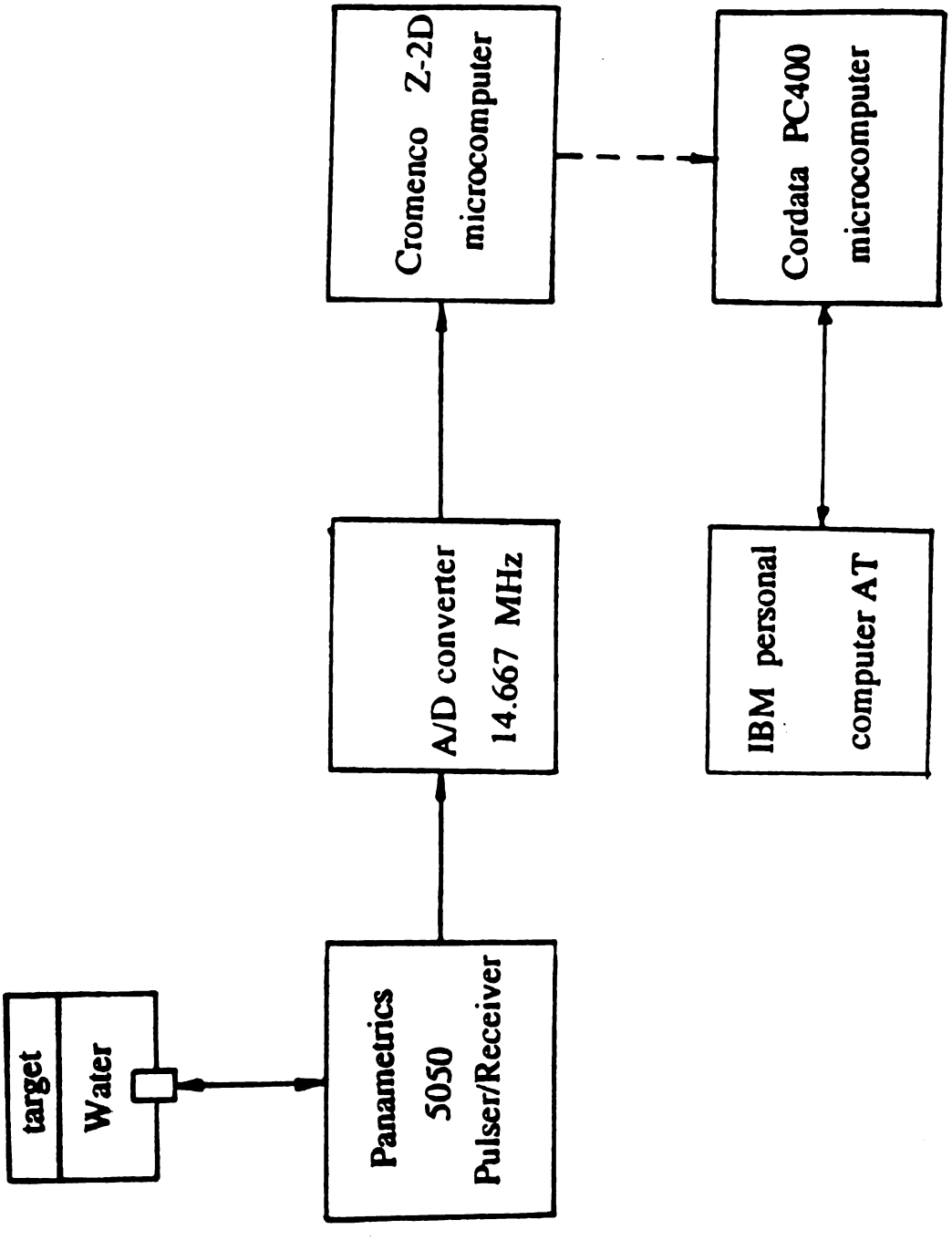

Figure 3.1.1 The block diagram of the experimental configurations

is as follows. The acoustic impedance of water is about 3650 times larger than that of air (refer to Table 2.2.1), the reflection coefficient of the water/air interface is practically equal to -1, that is, a complete reflection. For a short water path, the attenuation of ultrasound in water can be ignored. As a result, the reflected wave from water/air interface can be treated as the incident wave except the signal waveform is being inverted.

In the experiments, a transducer of frequency 2.25 MHz is used. A Panametrics 5050 Pulse Generator/Receiver is employed to generate pulse signals to the transducer and to receive the reflected signals.

In Figure 3.1.1, the signal is sampled by an A/D conversion circuit with a sampling rate of 14.667 MHz. The sampled data will be sent to a Cromemco Z-2D microcomputer, and be transferred to an IBM personal computer AT for further processing.

3.1.2 Sampling Reflected signal waveforms from objects

The reflected signals from an object under test can be obtained in a similar manner. That is, the transducer transmits an ultrasound pulse to the water/object interface and then receives the echoes. The reflected signal is sampled at 14.667 MHz and the sampled data is processed in a microcomputer to obtain the characteristics of the object.

3.2 Data processing

The signal received from the system shown in Figure 3.1.1 is the data in the time domain. These signals are transformed into the frequency domain. The reflection coefficients at different frequencies are calculated from the frequency components. Signal extraction is complicated by the fact that noise exists and by system jitter. Improvement in experimental accuracy is achieved by signal processing and by statistical methods. Software processing is preferred for high accuracy, while hardware circuitry is for fast processing.

Data processing consists of three main parts: correlation, averaging and spectral analysis.

3.2.1 Correlation and averaging

A video pulse contains many frequency components. Every frequency component contributes information to the final result. Therefore, one should take as many frequency components as possible. However, if too wide a band is taken, noise will be overwhelming. One way to increase the signal-to-noise ratio is to use averaging of multiple returns. The zero mean stationary noise is averaged to zero so that the signal-to-noise ratio will increase by $\sqrt{N}$ if N signals are averaged.

Noise reduction results from averaging and also from signal matching. Due to the system uncertainty (jitter), the phase of each signal is different. Thus signal phase alignment is necessary before signal averaging. The phase difference of two signals can be detected by calculating the correlation between them. The position of the peak value of the correlation function will be the distance between these two signals. After the distance between two signals has been detected, one can be aligned in order to do the averaging.

We will use a real experimental example to show how the correlation and average work. Figures (3.2.1) and (3.2.2) are two original waveforms reflected from a water/aluminum interface. It can be seen that these waveforms have significant noise present. In order to reduce the noise, the correlation is calculated as shown in Figure 3.2.3 to find the distance between them. Based on the calculated distance, waveform (2) can be shifted and averaged with waveform (1). For a twelve waveform correlation and average, the resultant waveform is shown in Figure (3.2.6). The average waveform is smoother and contains less noise. Comparing the spectrum of each waveform (Figures (3.2.4), (3.2.5), and (3.2.7)-(3.2.9)), we see at the high frequency noise is filtered by the averaging process. Thus correlation and averaging are excellent techniques for increasing the signal-to-noise ratio.

Fourier Transform and inverse Fourier Transform

After the signal averaging process is completed, the frequency spectra of the signal is obtained from its Fourier transform. A general purpose Fast Fourier Transform routine was developed for calculating the spectrum and displaying the phase as well as the magnitude of each frequency component. In addition, some weighting windows may be added to further improve the results. The weighting windows includes various types, such as the rectangular, triangular, Hamming, and Hanning windows. In addition to the Fourier Transform, the inverse Fourier Transform is avaliable for time domain representation.

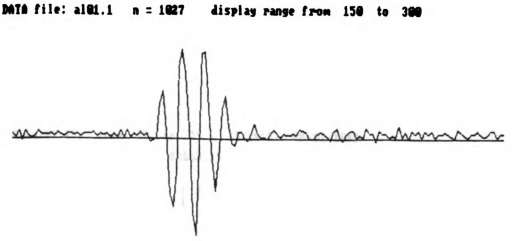

Figure 3.2.1 The waveform(1) reflected from water/aluminum interface

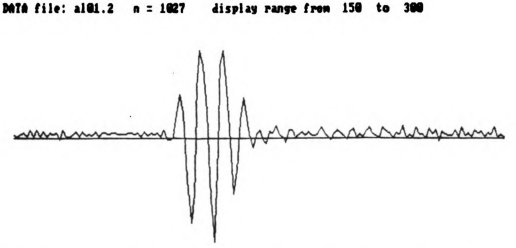

Figure 3.2.2 The waveform(2) reflected from water/aluminum interface

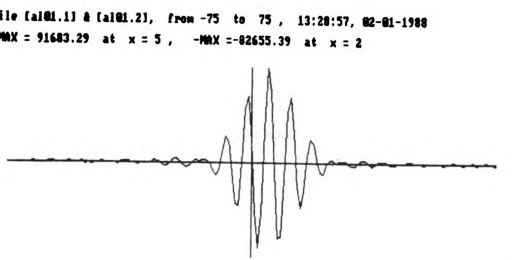

Figure 3.2.3 The correlation of waveform(1) and waveform(2)

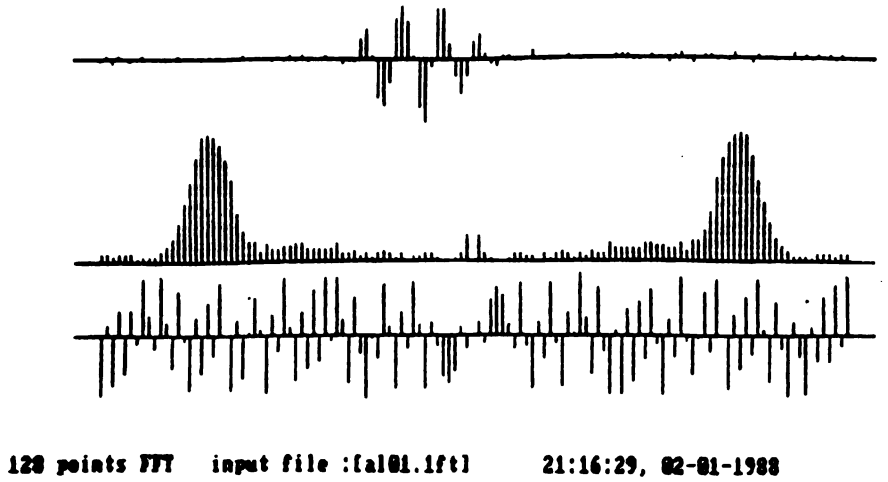

Figure 3.2.4 The spectrum of waveform(1)

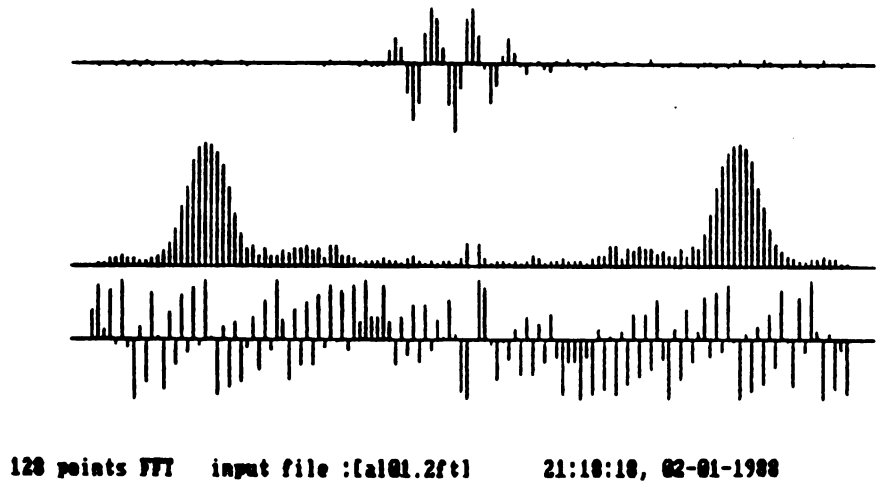

Figure 3.2.5 The spectrum of waveform(2)

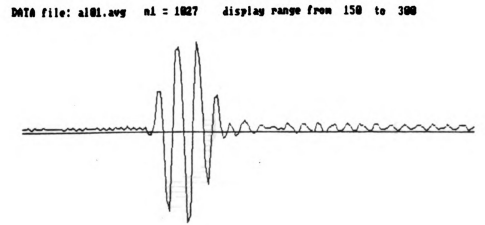

Figure 3.2.6 The average waveform reflected from water/aluminum interface

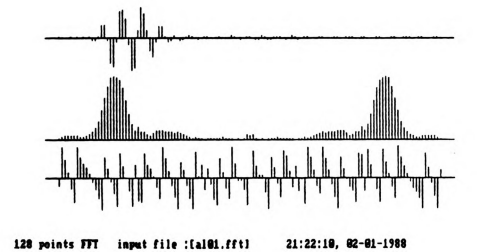

Figure 3.2.7 The spectrum of average waveform

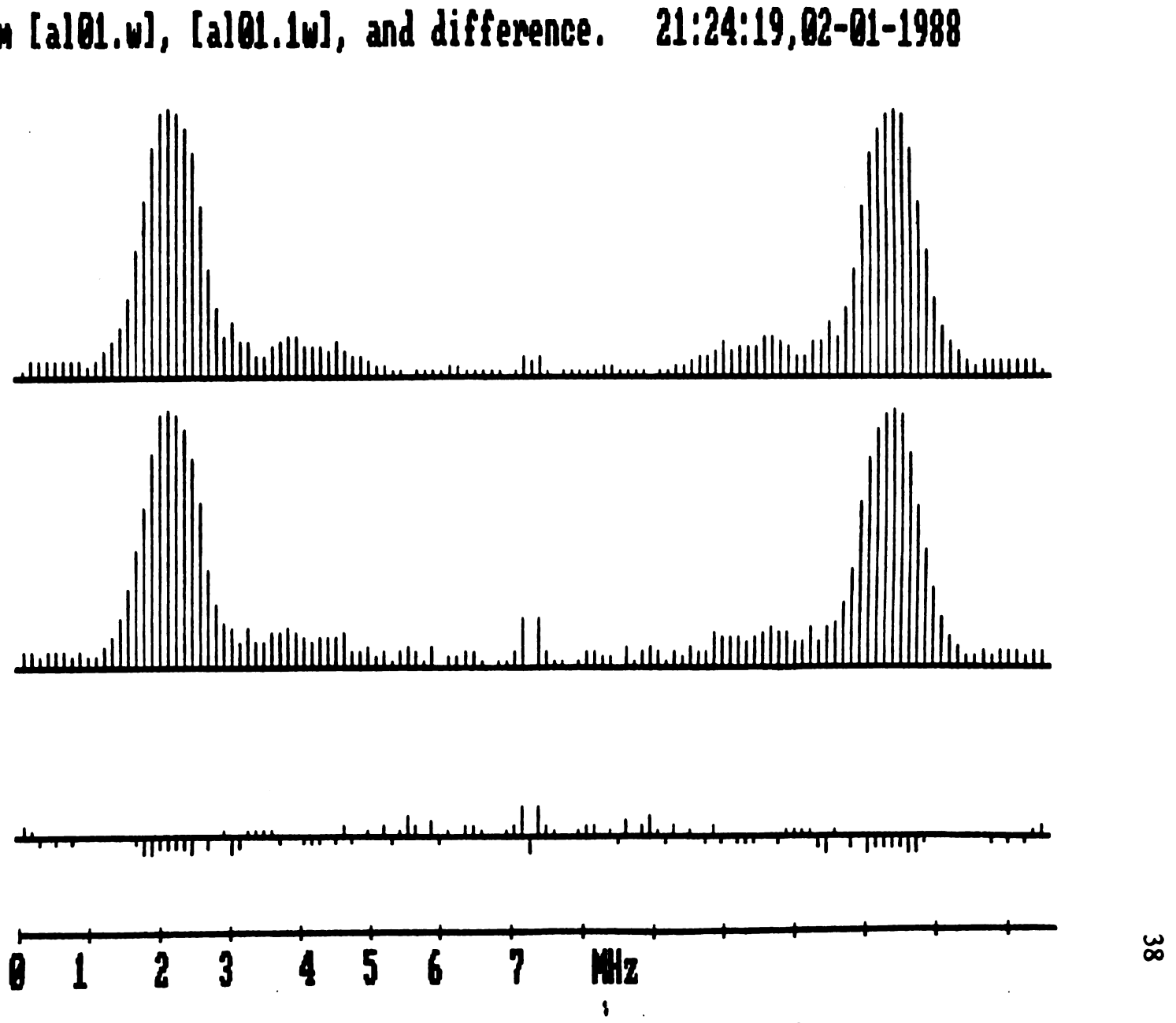

Figure 3.2.8 The spectral difference between the waveform(1) and the average waveform spectra

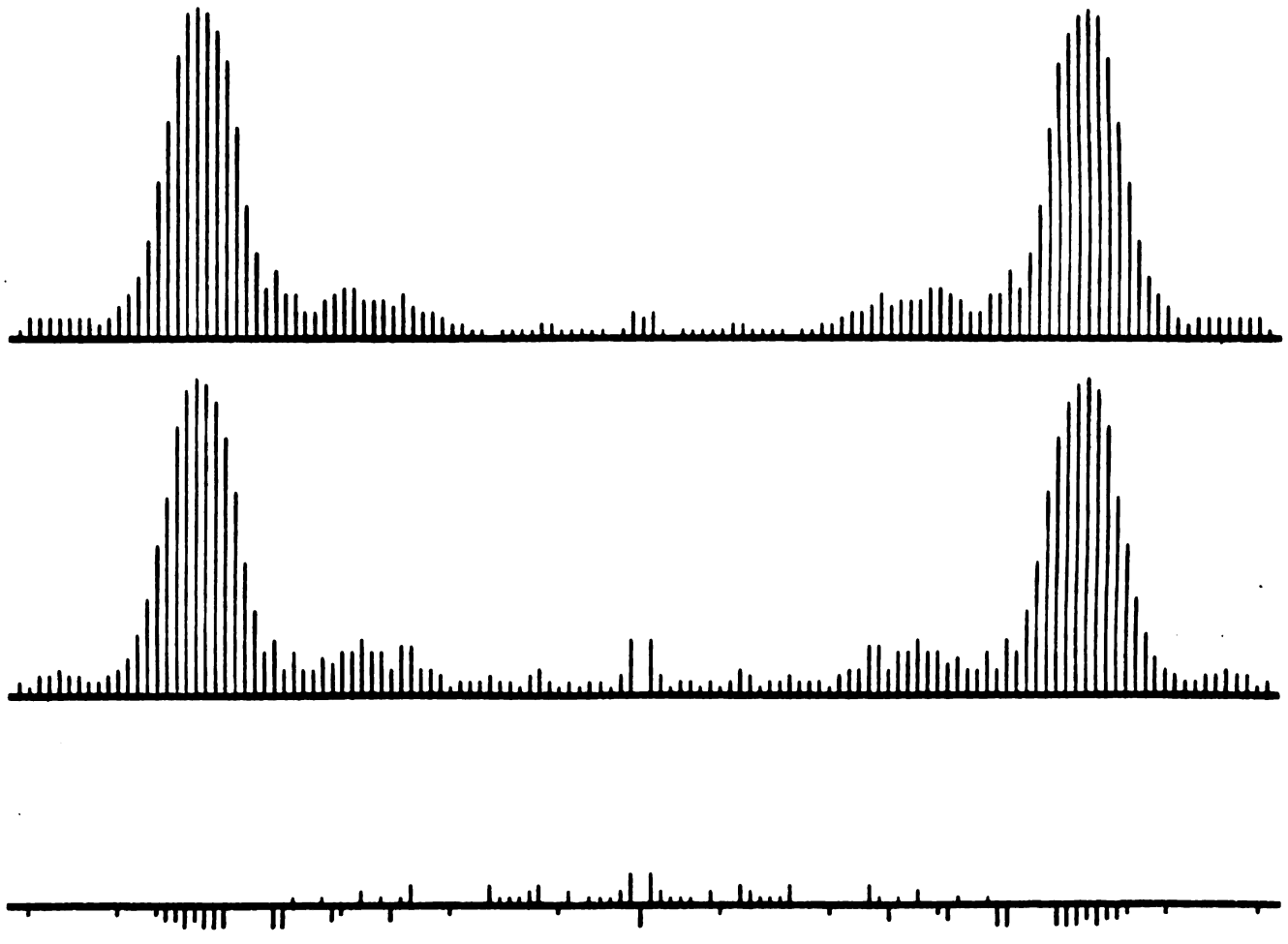

Figure 3.2.9 The spectral difference between the waveform(2) and the average waveform spectra

CHAPTER 4

Analysis of Experimental Results

The experimental results obtained from the system described in chapter 3 are listed in section 4.1. The characteristics of each tested material are analyzed in section 4.2. In section 4.3, some conclusions are provided and suggestions for future study presented.

4.1 Experimental Results

4.1.1 The Incident Signal

Using the setup in Figure 3.1.1 and the method described in section 3.1.1, the inverse incident waveform was obtained and shown in Figure 4.1.1. The waveform in Figure 4.1.1 is an averaged waveform of twelve reflections from the water/air interface. Figure 4.1.3 is the spectrum of the averaged incident waveform. It is observed that about 90 percent of the energy is within the frequency band from 1 MHz to 5 MHz.

In order to ensure that the experimental results are repeatable, the reflected signal from the water/air interface was measured on different days. Figure 4.1.2 is the average of eight waveforms and Figure 4.1.4 shows its spectrum. The results of the second set of data is very close to the first. In

addition to comparing the signal in the time domain, we can also compare them in the frequency domain (Figure 4.1.5). The spectral difference between the two appears to be small. In other words, the experimental results are time independent and repeatable.

4.1.2 The Signals reflected from Tested Materials

Several materials are tested by the video pulse system. They are aluminum, plexiglass, composite material, wood, rubber and stone. Both the reflected waveforms and the spectrum of each material are shown in Figures (4.1.6)-(4.1.17).

4.2 Discussion

In order to reduce noise from the return signal, twelve reflected waveforms from the same target were averaged to increase the signal-to-noise ratio by $\sqrt{12} \approx 3.464$. This process proved to be extremely valuable.

In chapter 2, we have shown that the reflection coefficient can be expressed in terms of material densities and wave propagation constants as, Eq. (2.3.8),

$$R = \frac{K_1\rho_2 - K_2\rho_1}{K_1\rho_2 + K_2\rho_1} \tag{4.2.1}$$

where $K = \beta - j\alpha$.

```
12:55:46   01-28-1988
Data file =air02
No. of files,  n = 12
Correlation range from    200    to    350
Max difference between two data file    dmax =? 50

The distance between [air02.2] and [air02.avg] is  4 with  cmax = 86385
The distance between [air02.3] and [air02.avg] is  3 with  cmax = 89646
The distance between [air02.4] and [air02.avg] is  5 with  cmax = 85249
The distance between [air02.5] and [air02.avg] is  7 with  cmax = 83110.5
The distance between [air02.6] and [air02.avg] is  6 with  cmax = 86301.98
The distance between [air02.7] and [air02.avg] is -4 with  cmax = 89236.3
The distance between [air02.8] and [air02.avg] is -1 with  cmax = 84794.09
The distance between [air02.9] and [air02.avg] is  5 with  cmax = 83125.5
The distance between [air02.10] and [air02.avg] is  9 with  cmax = 86480.1
The distance between [air02.11] and [air02.avg] is -3 with  cmax = 89371.02
The distance between [air02.12] and [air02.avg] is  7 with  cmax = 85661.79
DATA file: air02.avg   ni = 1026    display range from 200 to 350
```

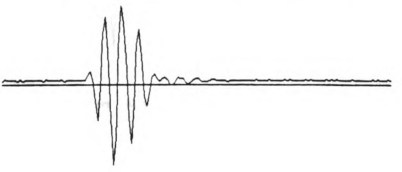

```
DATA file: air02.avg   ni = 1026    display range from 100 to 700
```

Figure 4.1.1 The waveform reflected from water/air interface
(the incident signal)

```
14:59:40   01-28-1988
Data file =air03
No. of files,  n = 8
Correlation range from   200   to   350
Max difference between two data file   dmax =? 50

The distance between [air03.2] and [air03.avg] is  7 with  cmax = 92441
The distance between [air03.3] and [air03.avg] is  10 with  cmax = 87689
The distance between [air03.4] and [air03.avg] is  10 with  cmax = 88168.67
The distance between [air03.5] and [air03.avg] is  8 with  cmax = 83342
The distance between [air03.6] and [air03.avg] is  7 with  cmax = 90498.42
The distance between [air03.7] and [air03.avg] is  7 with  cmax = 91774.5
The distance between [air03.8] and [air03.avg] is  12 with  cmax = 90769.45
DATA file: air03.avg  ni = 1026   display range from 200 to 350
```

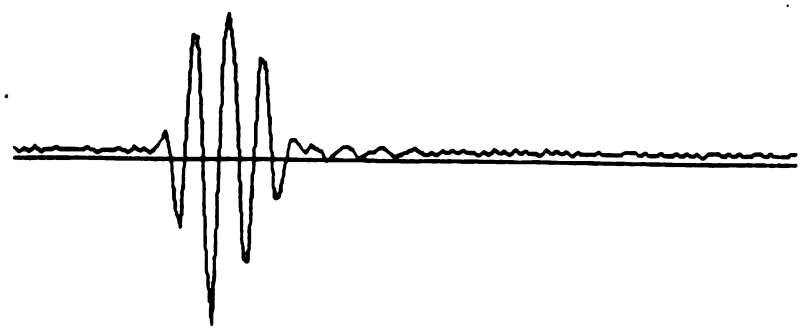

```
DATA file: air03.avg  ni = 1026   display range from 100 to 700
```

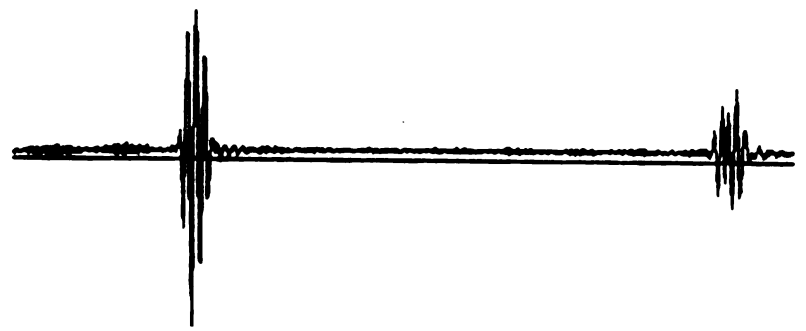

Figure 4.1.2 The waveform reflected from water/air interface

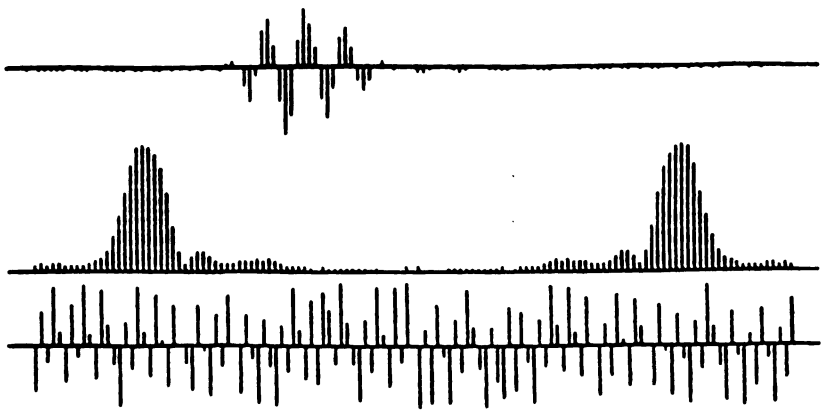

Figure 4.1.3 The spectrum of incident signal

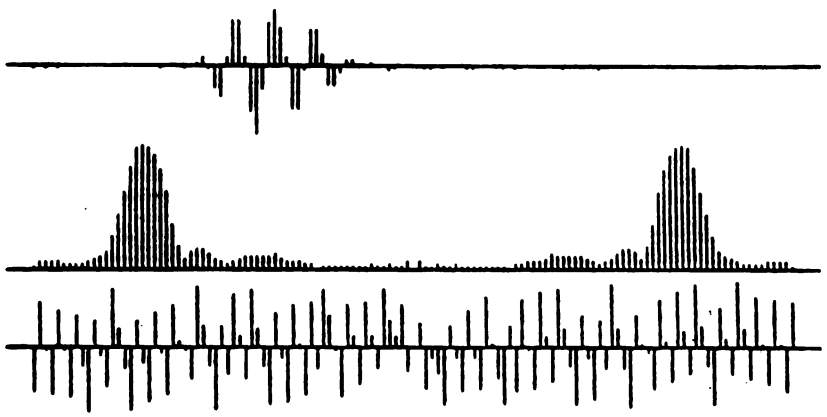

Figure 4.1.4 The spectrum of waveform reflected from water/air interface

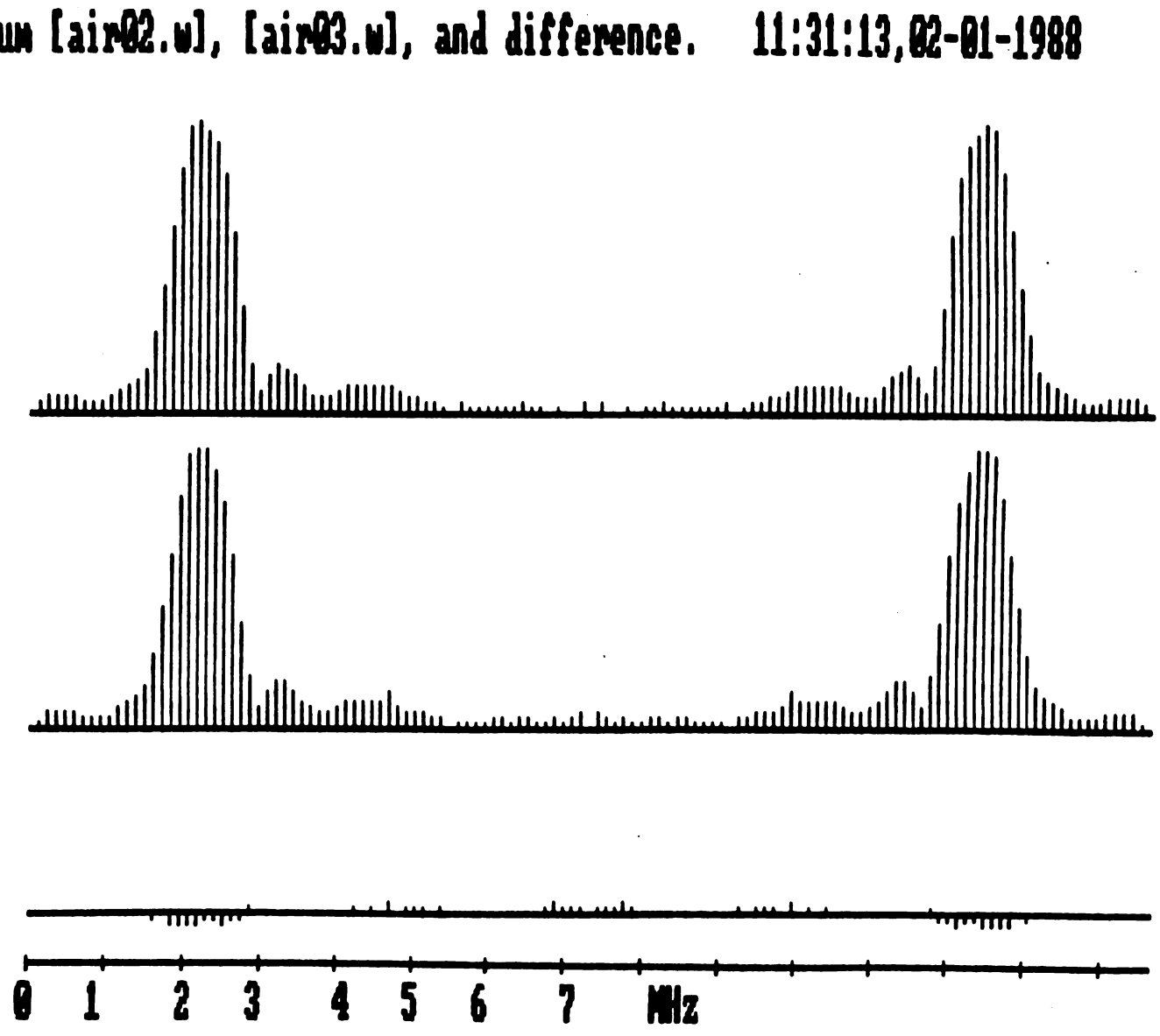

Figure 4.1.5 The spectrum difference between incidence and water/air reflection

```
11:54:43   01-18-1988
Data file =al01
No. of files,  n = 12
Correlation range from   150   to   300
Max difference between two data file   dmax =? 50

The distance between [al01.2] and [al01.avg] is  5 with  cmax = 96297
The distance between [al01.3] and [al01.avg] is  1 with  cmax = 87583.5
The distance between [al01.4] and [al01.avg] is -13 with  cmax = 95326.33
The distance between [al01.5] and [al01.avg] is  9 with  cmax = 95472.75
The distance between [al01.6] and [al01.avg] is  9 with  cmax = 92636.2
The distance between [al01.7] and [al01.avg] is  5 with  cmax = 95707.49
The distance between [al01.8] and [al01.avg] is  9 with  cmax = 96216.43
The distance between [al01.9] and [al01.avg] is -1 with  cmax = 95108
The distance between [al01.10] and [al01.avg] is  3 with  cmax = 86399.66
The distance between [al01.11] and [al01.avg] is  7 with  cmax = 94257.91
The distance between [al01.12] and [al01.avg] is  1 with  cmax = 92187.16
DATA file: al01.avg  ni = 1027   display range from 150 to 300
```

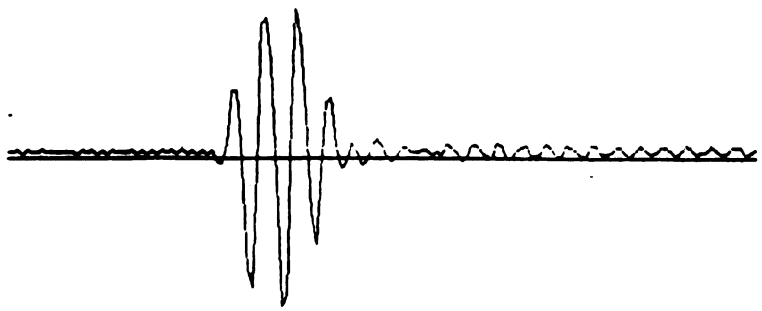

```
DATA file: al01.avg  ni = 1027   display range from 100 to 700
```

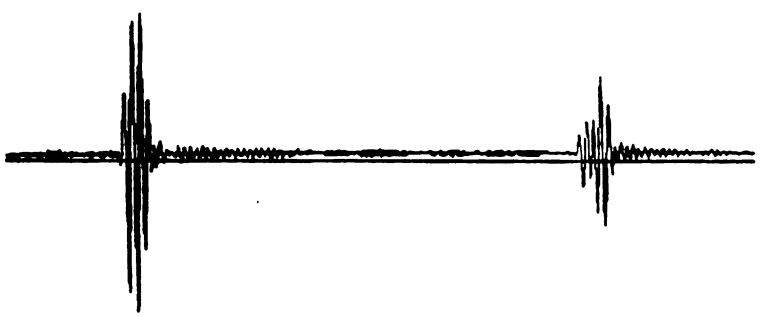

Figure 4.1.6 The waveform reflected from water/aluminum interface

```
14:46:34   01-27-1988
Data file =pglass01
No. of files,  n = 12
Correlation range from   200   to   350
Max difference between two data file   dmax =? 50

The distance between [pglass01.2] and [pglass01.avg] is  5 with  cmax = 27186
The distance between [pglass01.3] and [pglass01.avg] is  14 with  cmax =
 27582.5
The distance between [pglass01.4] and [pglass01.avg] is -19 with  cmax =
 27020.01
The distance between [pglass01.5] and [pglass01.avg] is -7 with  cmax = 27662

The distance between [pglass01.6] and [pglass01.avg] is  3 with  cmax =
 27036.79
The distance between [pglass01.7] and [pglass01.avg] is  7 with  cmax =
 27845.67
The distance between [pglass01.8] and [pglass01.avg] is -9 with  cmax =
 25183.29
The distance between [pglass01.9] and [pglass01.avg] is -2 with  cmax =
 26006.75
The distance between [pglass01.10] and [pglass01.avg] is  12 with  cmax =
 27112.44
The distance between [pglass01.11] and [pglass01.avg] is  8 with  cmax =
 27120.7
The distance between [pglass01.12] and [pglass01.avg] is  13 with  cmax =
 25779.36
DATA file: pglass01.avg  ni = 1026  display range from 200 to 350
```

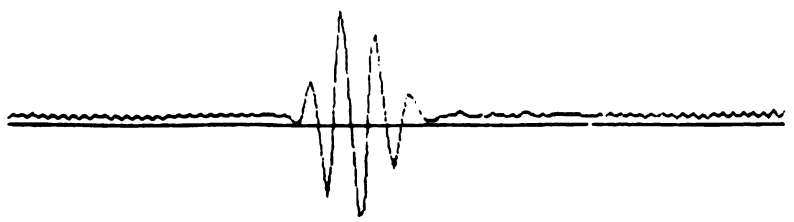

```
DATA file: pglass01.avg  ni = 1026  display range from 100 to 700
```

Figure 4.1.7 The waveform reflected from water/plexigalss interface

```
12:28:37   02-01-1988
Data file =comp02
No. of files,  n = 12
Correlation range from   200   to   350
Max difference between two data file   dmax =? 20

The distance between [comp02.2] and [comp02.avg] is  10 with  cmax = 32390
The distance between [comp02.3] and [comp02.avg] is  5 with  cmax = 30313
The distance between [comp02.4] and [comp02.avg] is  3 with  cmax = 32401.33
The distance between [comp02.5] and [comp02.avg] is  9 with  cmax = 32156.75
The distance between [comp02.6] and [comp02.avg] is  8 with  cmax = 31794.79
The distance between [comp02.7] and [comp02.avg] is  7 with  cmax = 33269.5
The distance between [comp02.8] and [comp02.avg] is  13 with  cmax = 30801.29
The distance between [comp02.9] and [comp02.avg] is  13 with  cmax = 30539.13
The distance between [comp02.10] and [comp02.avg] is  11 with  cmax = 32910
The distance between [comp02.11] and [comp02.avg] is -18 with  cmax = 32840.8
The distance between [comp02.12] and [comp02.avg] is  9 with  cmax = 30293.83
DATA file: comp02.avg  ni = 1027  display range from 200 to 350
```

```
DATA file: comp02.avg  ni = 1027  display range from 100 to 700
```

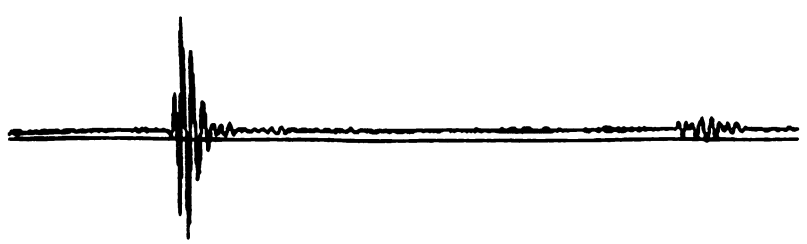

Figure 4.1.8 The waveform reflected from water/composite material interface

```
13:02:18   02-01-1988
Data file =wood01
No. of files,  n = 12
Correlation range from   200   to   350
Max difference between two data file   dmax =? 10

The distance between [wood01.2] and [wood01.avg] is  0 with  cmax = 34089
The distance between [wood01.3] and [wood01.avg] is  4 with  cmax = 32275.5
The distance between [wood01.4] and [wood01.avg] is  4 with  cmax = 35639.99
The distance between [wood01.5] and [wood01.avg] is  0 with  cmax = 35272.5
The distance between [wood01.6] and [wood01.avg] is  3 with  cmax = 33639.62
The distance between [wood01.7] and [wood01.avg] is -1 with  cmax = 32888.17
The distance between [wood01.8] and [wood01.avg] is  7 with  cmax = 35159.99
The distance between [wood01.9] and [wood01.avg] is -5 with  cmax = 35866
The distance between [wood01.10] and [wood01.avg] is  3 with  cmax = 35641.89
The distance between [wood01.11] and [wood01.avg] is  8 with  cmax = 33395.1
The distance between [wood01.12] and [wood01.avg] is  4 with  cmax = 36560.54
DATA file: wood01.avg  ni = 1027   display range from 200 to 350
```

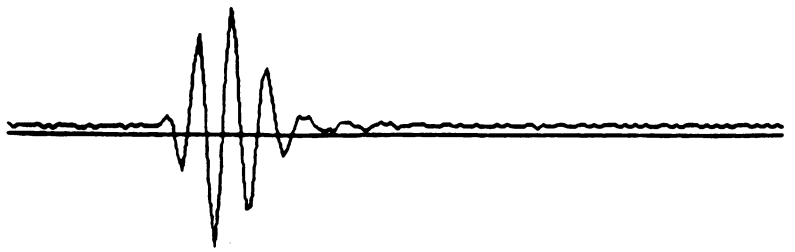

```
DATA file: wood01.avg  ni = 1027   display range from 100 to 700
```

Figure 4.1.9 The waveform reflected from water/wood interface

```
12:19:08   02-01-1988
Data file =rub02
No. of files,  n = 12
Correlation range from   200   to   350
Max difference between two data file   dmax =? 40

The distance between [rub02.2] and [rub02.avg] is  0 with  cmax = 42174
The distance between [rub02.3] and [rub02.avg] is -15 with  cmax = 43782
The distance between [rub02.4] and [rub02.avg] is -4 with  cmax = 40974.33
The distance between [rub02.5] and [rub02.avg] is -17 with  cmax = 40989
The distance between [rub02.6] and [rub02.avg] is -1 with  cmax = 39868
The distance between [rub02.7] and [rub02.avg] is -20 with  cmax = 40999.34
The distance between [rub02.8] and [rub02.avg] is -8 with  cmax = 36785.29
The distance between [rub02.9] and [rub02.avg] is -2 with  cmax = 37717.5
The distance between [rub02.10] and [rub02.avg] is -36 with  cmax = 39757.55
The distance between [rub02.11] and [rub02.avg] is -6 with  cmax = 37525.2
The distance between [rub02.12] and [rub02.avg] is  2 with  cmax = 37581.1
DATA file: rub02.avg  ni = 1027   display range from 200 to 350
```

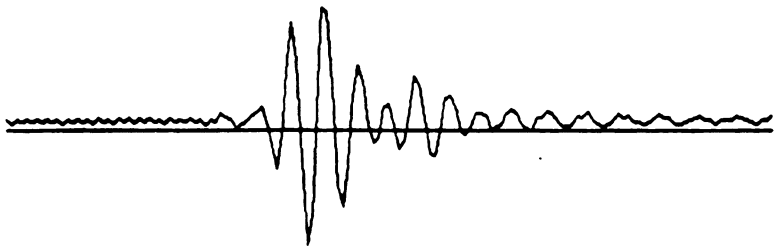

```
DATA file: rub02.avg  ni = 1027   display range from 150 to 750
```

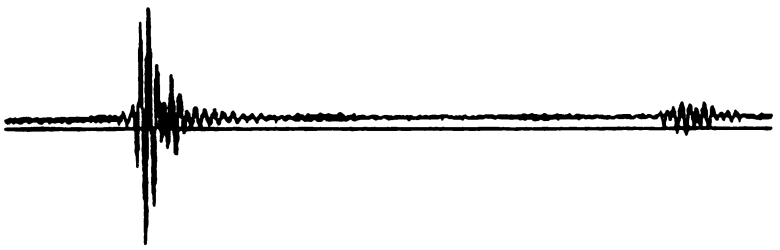

Figure 4.1.10 The waveform reflected from water/rubber interface

```
12:49:14   02-01-1988
Data file =stone01
No. of files,  n = 12
Correlation range from   200   to   350
Max difference between two data file   dmax =? 80

The distance between [stone01.2] and [stone01.avg] is  0 with  cmax = 88899
The distance between [stone01.3] and [stone01.avg] is -52 with  cmax = 92041
The distance between [stone01.4] and [stone01.avg] is -56 with  cmax = 92744.3
                    .
The distance between [stone01.5] and [stone01.avg] is -42 with  cmax = 85527.2

The distance between [stone01.6] and [stone01.avg] is -39 with  cmax = 87300.0

The distance between [stone01.7] and [stone01.avg] is -38 with  cmax = 88888.5
The distance between [stone01.8] and [stone01.avg] is -4 with  cmax = 87038.68
The distance between [stone01.9] and [stone01.avg] is -3 with  cmax = 91152.1
The distance between [stone01.10] and [stone01.avg] is  2 with  cmax = 89838.1

The distance between [stone01.11] and [stone01.avg] is -12 with  cmax =
 92052.21
The distance between [stone01.12] and [stone01.avg] is  1 with  cmax = 90121.9
```

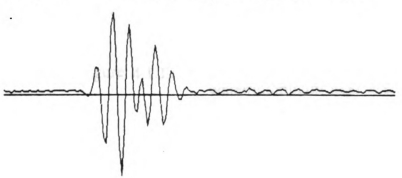

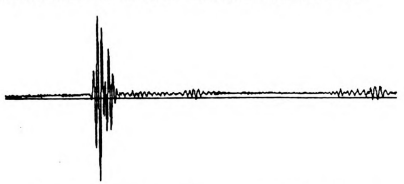

Figure 4.1.11 The waveform reflected from water/stone interface

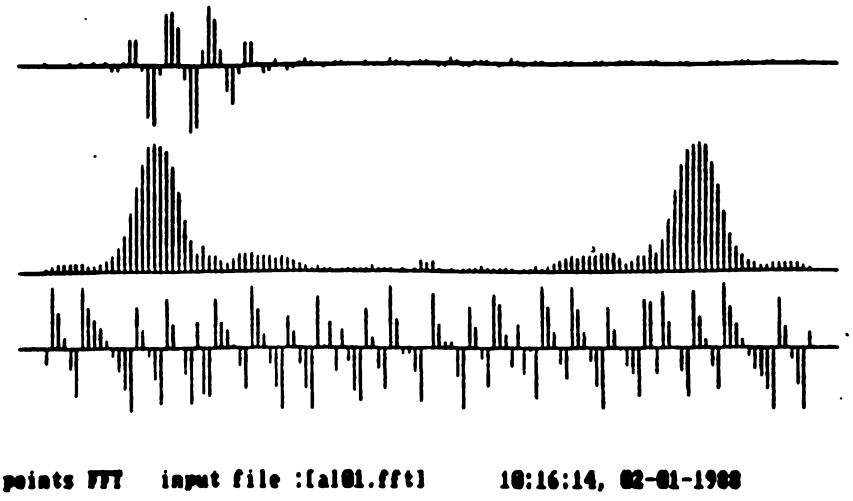

Figure 4.1.12 The spectrum of waveform reflected from water/aluminum interface

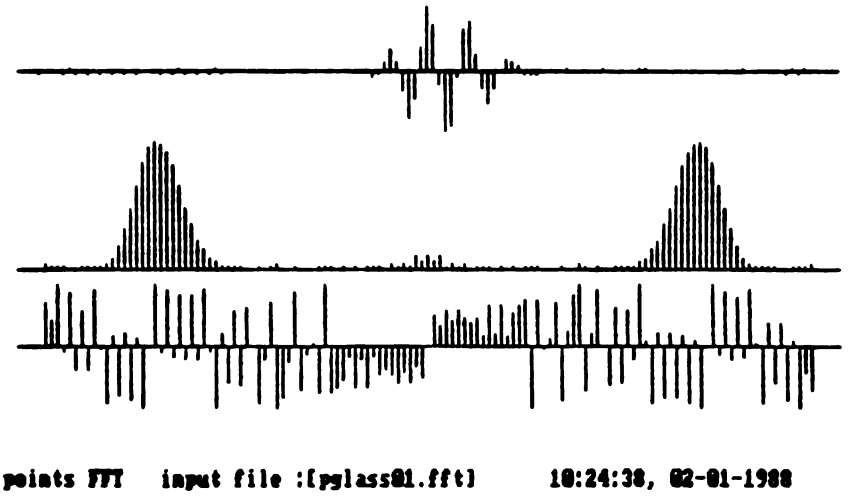

Figure 4.1.13 The spectrum of waveform reflected from water/plexigalss interface

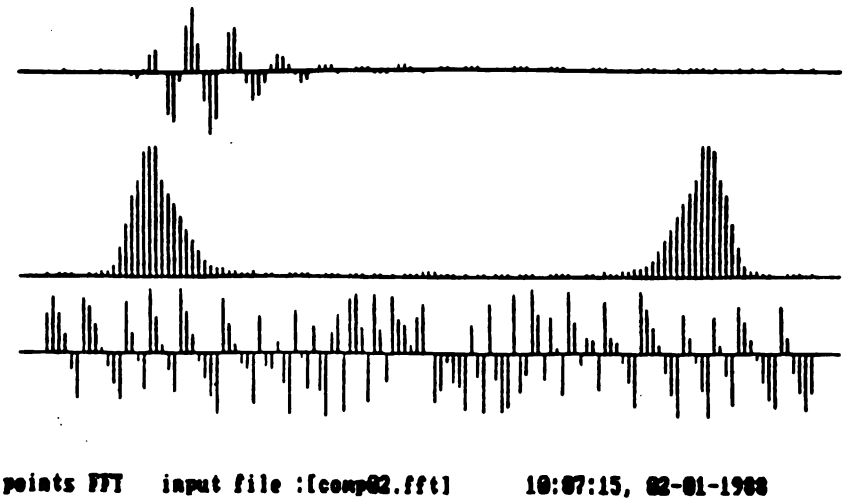

Figure 4.1.14 The spectrum of waveform reflected from water/composite material interface

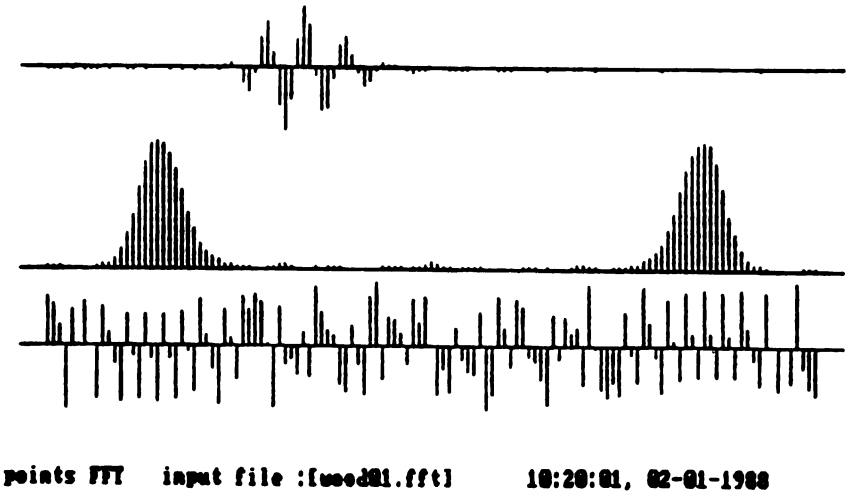

Figure 4.1.15 The spectrum of waveform reflected from water/wood interface

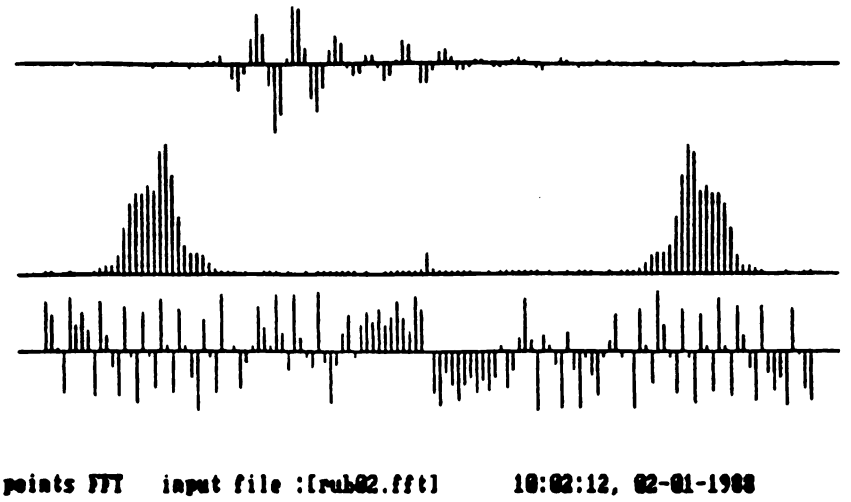

Figure 4.1.16 The spectrum of waveform reflected from water/rubber interface

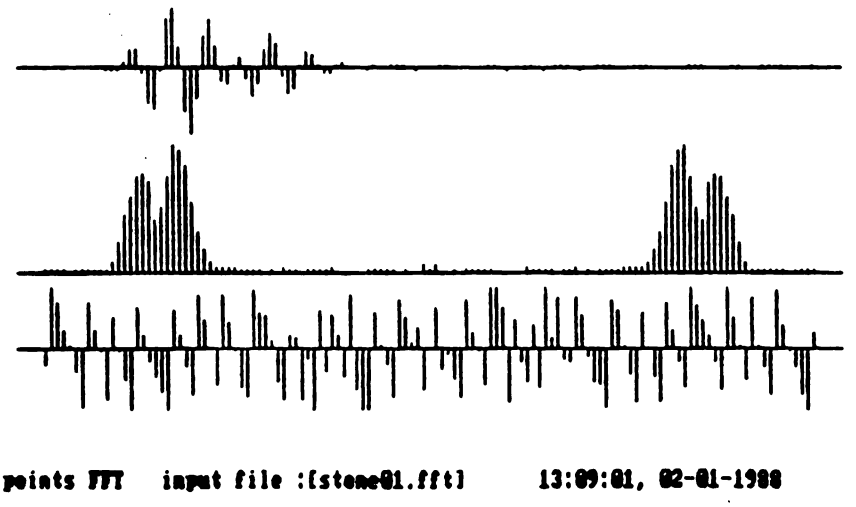

Figure 4.1.17 The spectrum of waveform reflected from water/stone interface

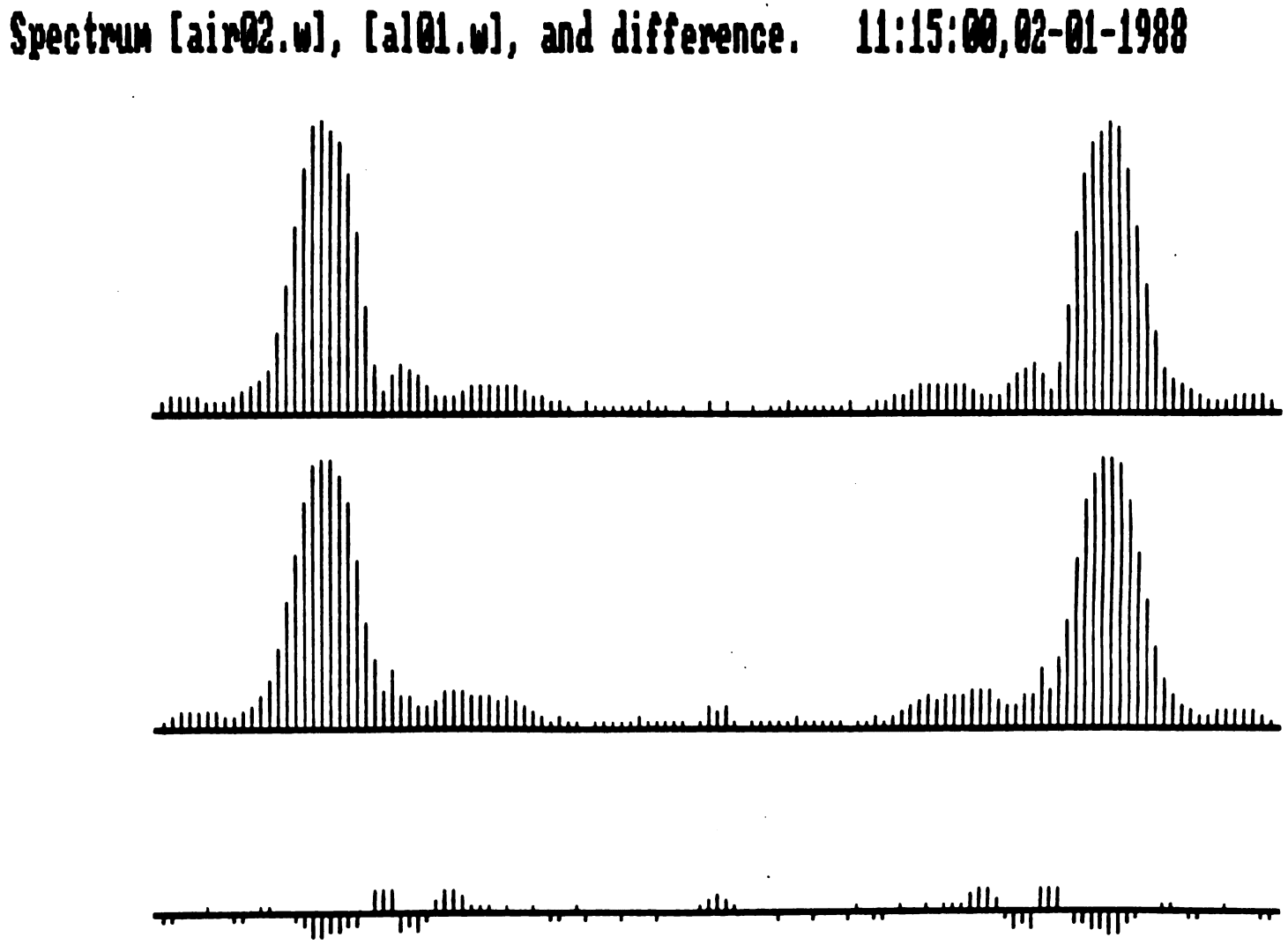

Figure 4.1.18 The spectral difference between incidence and water/aluminum reflection spectra

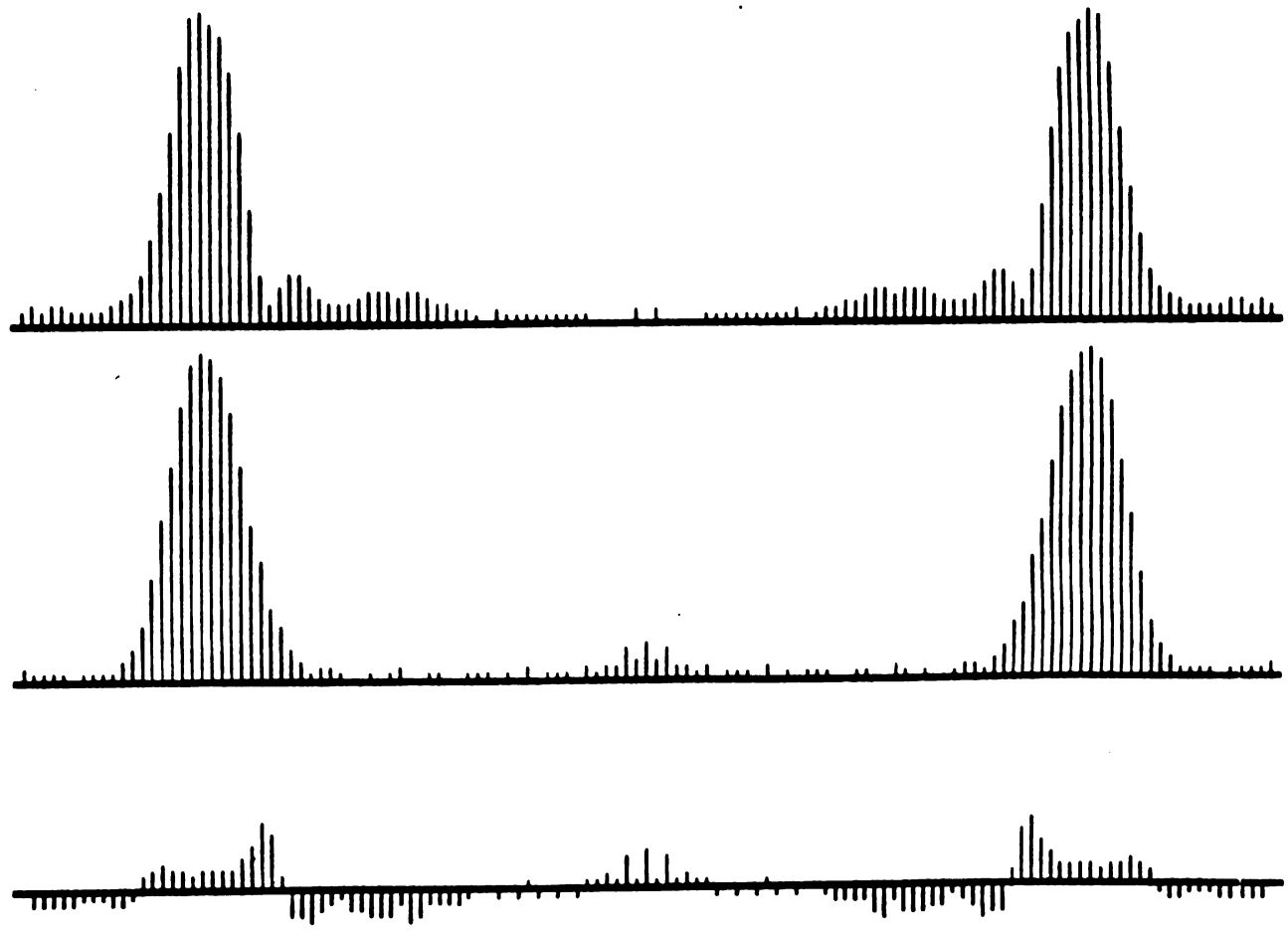

Figure 4.1.19 The spectral difference between incidence and water/plexiglass reflection spectra

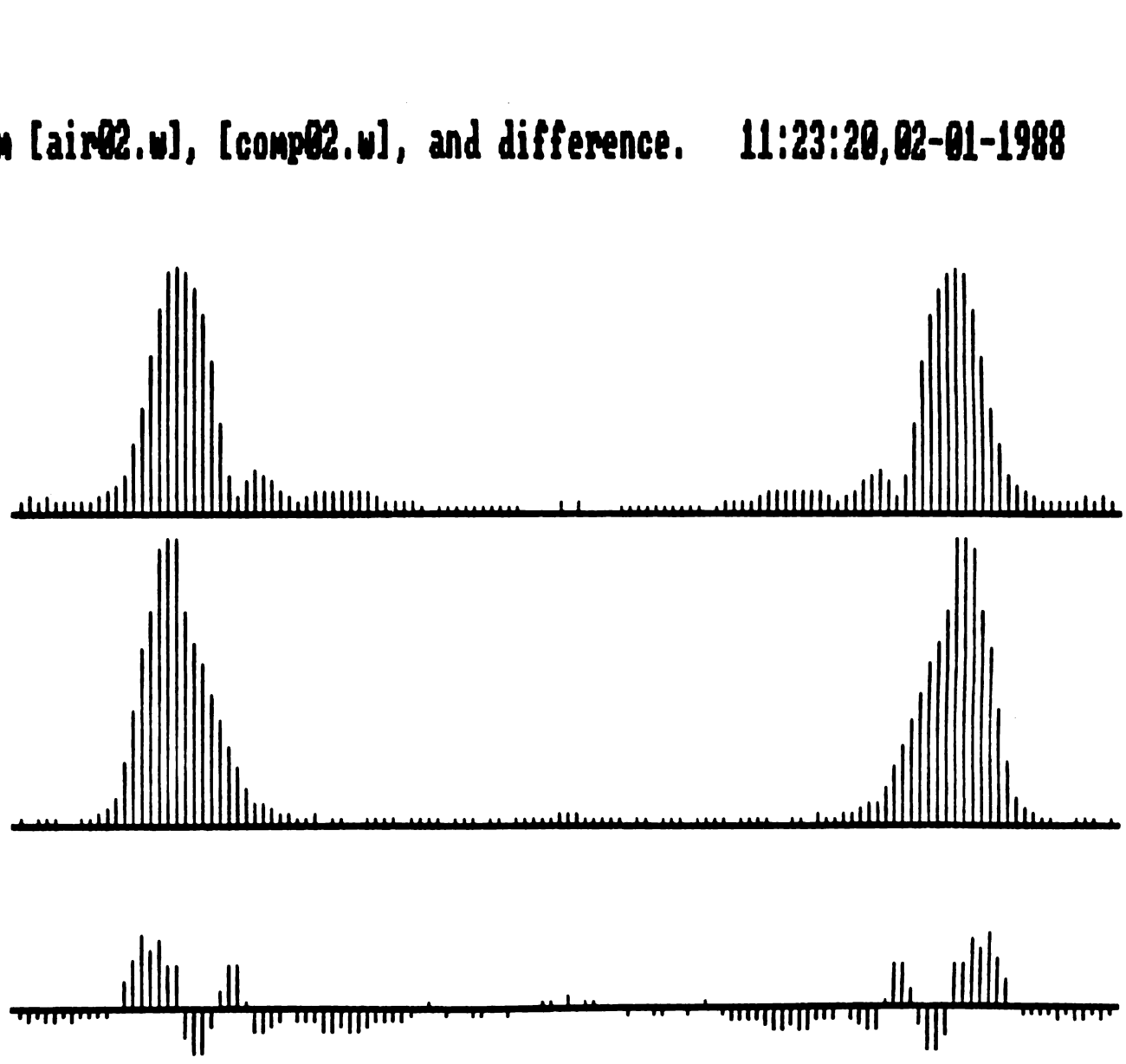

Figure 4.1.20 The spectral difference between incidence and water/composite material reflection spectra

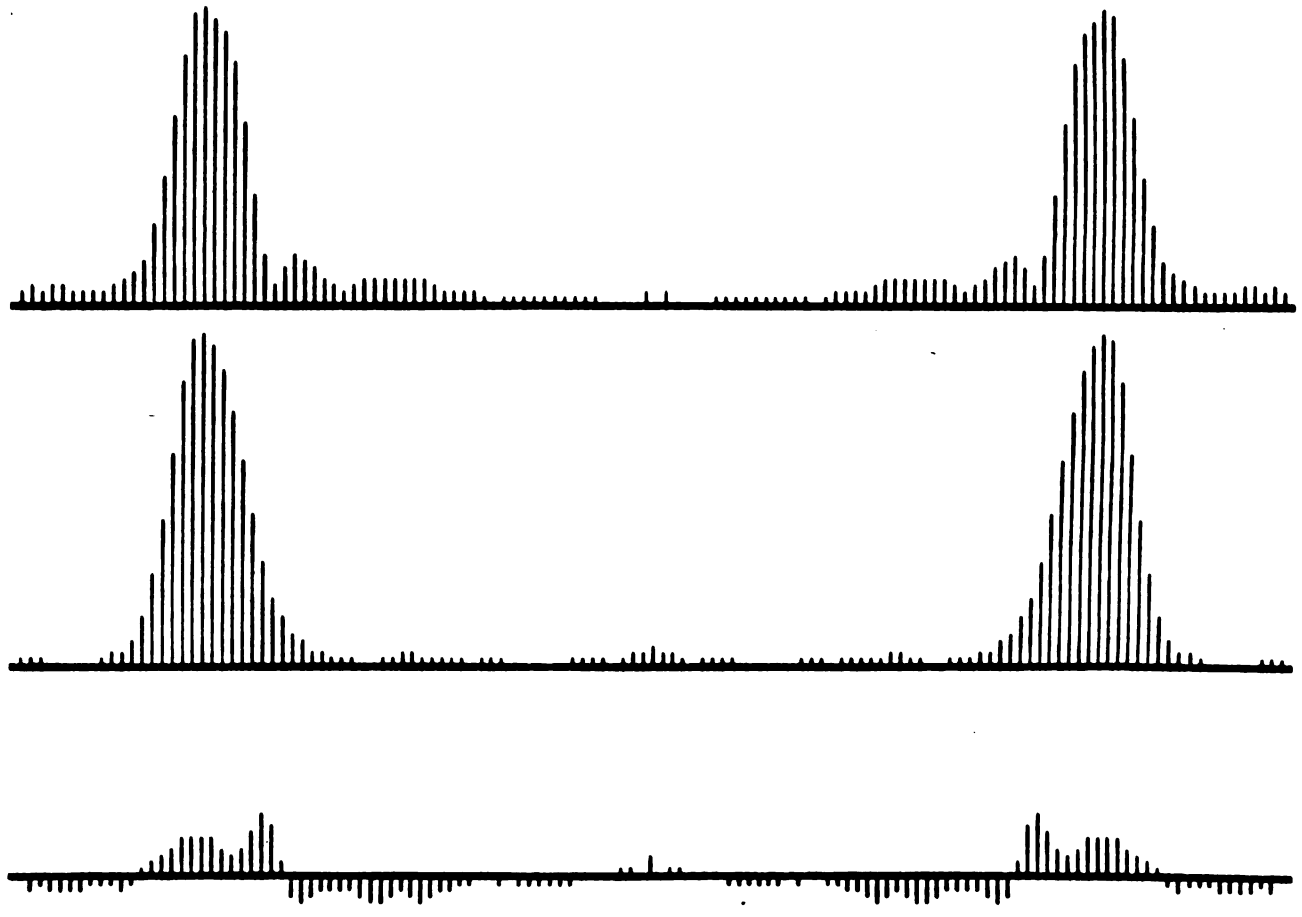

Figure 4.1.21 The spectral difference between incidence and water/wood reflection spectra

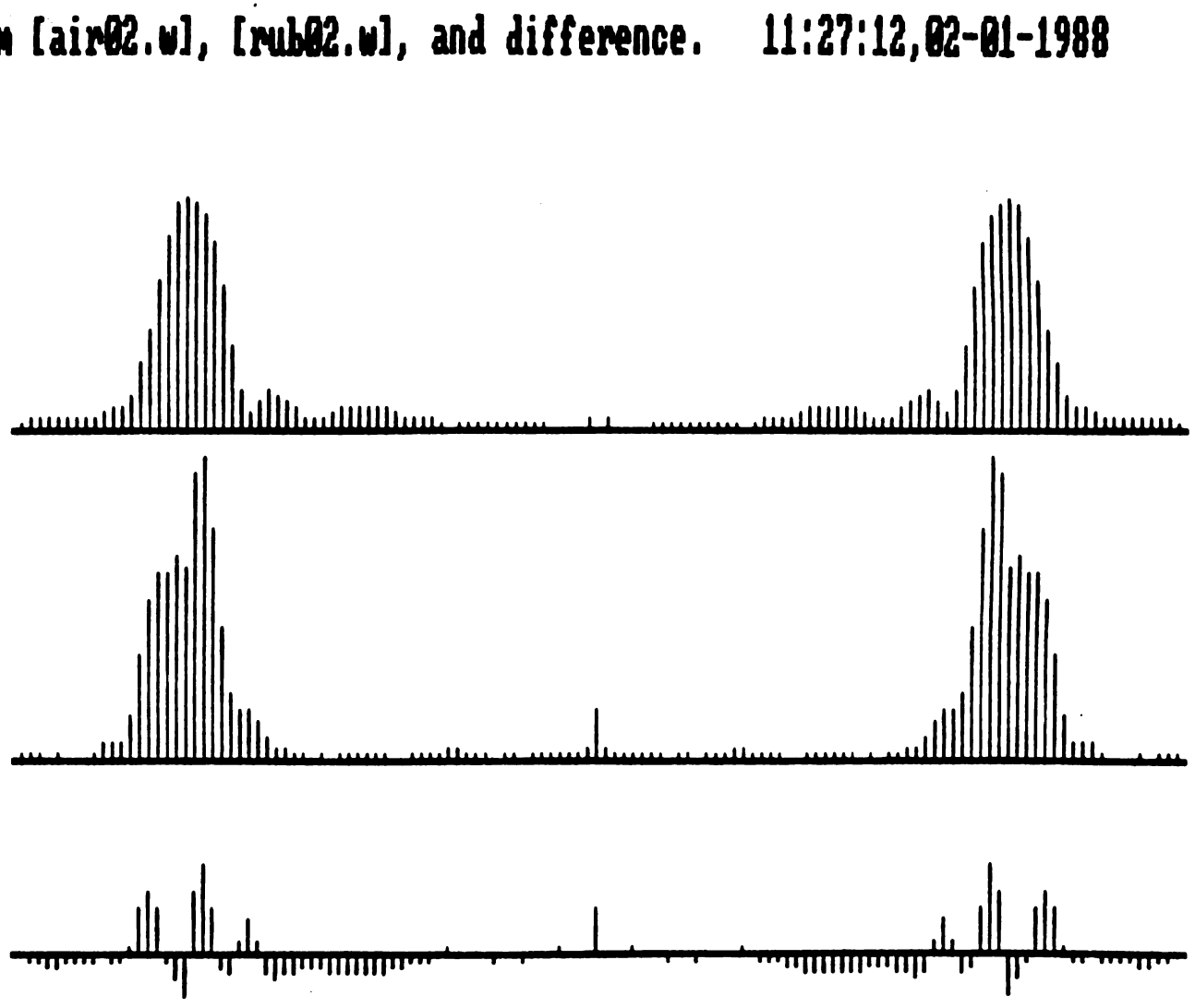

Figure 4.1.22 The spectral difference between incidence and water/rubber reflection spectra

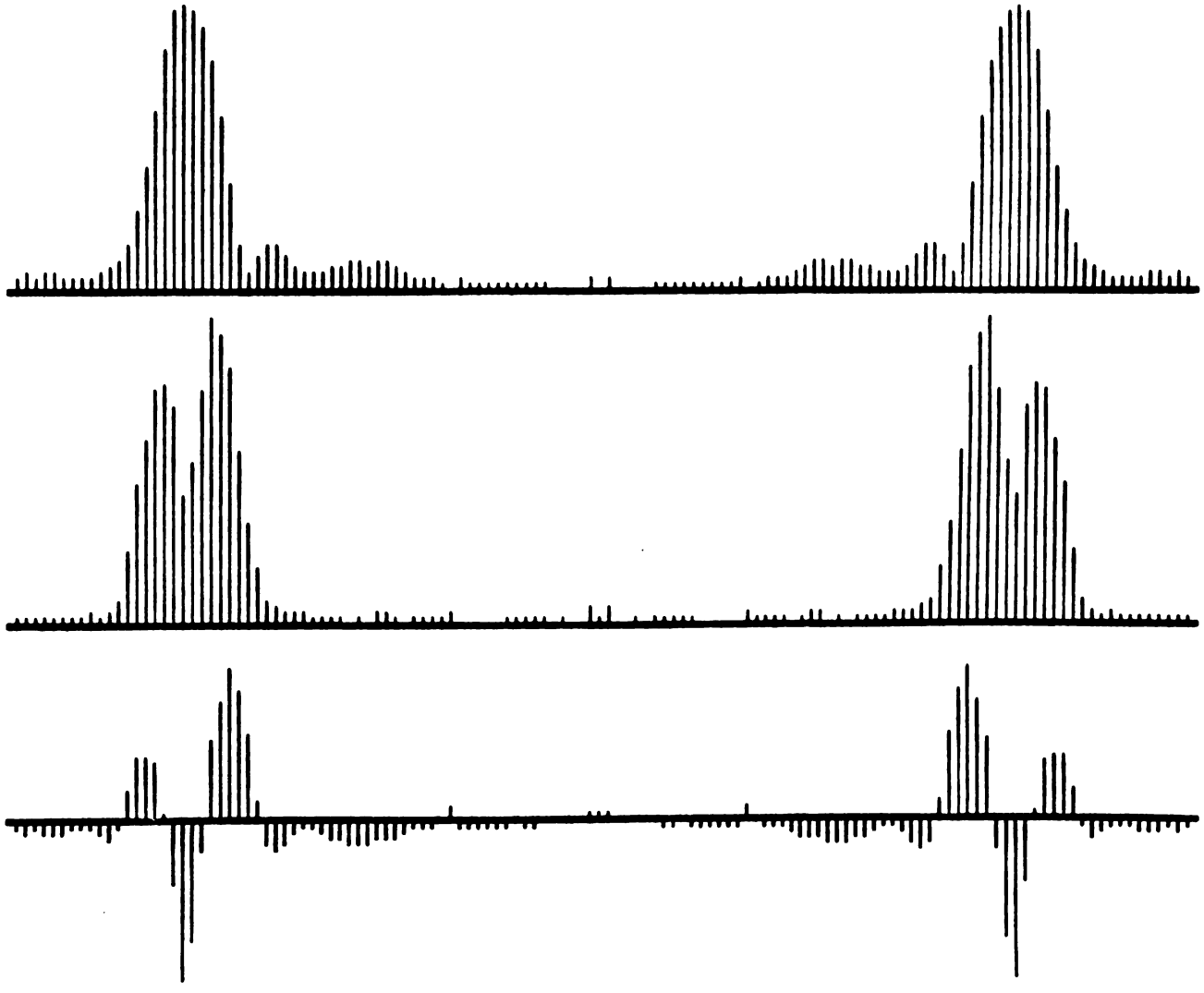

Figure 4.1.23 The spectral difference between incidence and water/stone reflection spectra

We have then,

$$R = \frac{(\beta_1\rho_2 - \beta_2\rho_1) - j(\alpha_1\rho_2 - \alpha_2\rho_1)}{(\beta_1\rho_2 + \beta_2\rho_1) - j(\alpha_1\rho_2 + \alpha_2\rho_1)} \tag{4.2.2}$$

When the operating frequency is low, or $(\frac{\eta\omega}{c})^2 << 1$, the attenuation coefficient α and phase constant β can be greatly simplified. From Eqs. (2.4.37) and (2.4.39), we have

$$\alpha \approx \frac{\eta\omega^2}{2c}\sqrt{\rho/c} \tag{4.2.3}$$

$$\beta \approx \omega\sqrt{\rho/c} \tag{4.2.4}$$

Then, the reflection coefficient becomes

$$R = \frac{[\sqrt{(\rho_2 c_2)/(\rho_1 c_1)} - 1] - j[\frac{\eta_1\omega}{2c_1}\sqrt{(\rho_2 c_2)/(\rho_1 c_1)} - \frac{\eta_2\omega}{2c_2}]}{[\sqrt{(\rho_2 c_2)/(\rho_1 c_1)} + 1] - j[\frac{\eta_1\omega}{2c_1}\sqrt{(\rho_2 c_2)/(\rho_1 c_1)} + \frac{\eta_2\omega}{2c_2}]} \tag{4.2.5}$$

Judging from this expression, the reflection coefficient R can be evaluated when the medium density ρ, elastic stiffness constant c, viscosity constant η and the operation frequency ω are known. The medium density and the acoustic propagation velocity for most materials are published. The elastic stiffness constant c can be obtained indirectly as follows:

The acoustic propagation velocity v is

$$v = \frac{\omega}{\beta} \tag{4.2.6}$$

Using the approximate value for phase constant β in Eq. (4.2.4), the velocity becomes

$$v \approx \sqrt{c/\rho} \tag{4.2.7}$$

With this, the elastic stiffness c becomes

$$c \approx \rho v^2 \tag{4.2.8}$$

An alternate way to obtain the viscosity constant is to use the attenuation expression of the medium (Eq.(2.4.30) or Eq.(4.2.3)).

Water was chosen as the first medium in our experiments. The density of water is $1000\, kg/m^3$ and the acoustic velocity is about $1500\, m/s$. Assuming no attenuation in water, the viscosity constant reduces to zero. The elastic stiffness constant is about $2.25\times10^9\, N/m^2$ from Eq. (4.2.8). With this stiffness constant, the reflection coefficient becomes:

$$R = \frac{[\sqrt{(\rho_2 c_2)/(2.25\times10^{12})} - 1] + j[\frac{\eta_2 \omega}{2c_2}]}{[\sqrt{(\rho_2 c_2)/(2.25\times10^{12})} + 1] - j[\frac{\eta_2 \omega}{2c_2}]} \tag{4.2.9}$$

In the following subsections, we will discuss the expermental results in three ways. 1) By comparing the signals in the time domain. 2) By comparing the spectral differences between the reflected waveform and the incident waveform, and 3) by determining the sign of the reflection coefficients.

4.2.1 Time domain signals

In the time domain it is easy to find the magnitude and damping of each signal. Figure 4.2.1 is the time domain representation of the signals for all materials tested. It can be seen that the magnitude and the damping of waveforms are different for different materials. For the signals in Figure 4.2.1, the power of each signal may be calculated by squaring the magnitude of the waveform. The mean value of the magnitude and the power of the first reflection of each signal is shown in Table 4.2.1.

Incident signal

From Table 2.2.1, the acoustic impedance of air is about 411 $kg/m^2 \cdot sec$ and that of water about 1.5×10^6 $kg/m^2 \cdot sec$. We may use Eq. (2.2.10) to get the reflection coefficient at the water/air interface, as:

$$R_{water/air} \approx -0.99945$$

which is very close to -1. Base on this, we can say that the signal reflected from the water/air interface is similar to the incident signal except the phase has been changed by 180^0.

In Table 4.2.1, we list two values for the reflected signals from the water/air interface. They are detected by the same setup but at different time. Theoretically, the power of the incident signal must be greater than

Table 4.2.1 The mean value of magnitude and power of the first reflection

Second medium	average magnitude	power of the first reflection
Air 1 (Incidence)	134.50	80946.57
Air 2	135.09	83813.83
Aluminum	133.77	89956.47
plexiglass	133.77	22289.42
composite material	133.71	27672.30
wood	133.62	30567.79
rubber	134.08	33940.06
stone	133.67	856.44

the power of the echo signals. It is surprising to see that the power of the water/aluminum reflection is greater than that of the water/air reflection. This may be due to the fact that the power of each incident signal is different or the the incident beam is not normal to the target surface, such that only part of the reflected power is received by the transducer. This may also

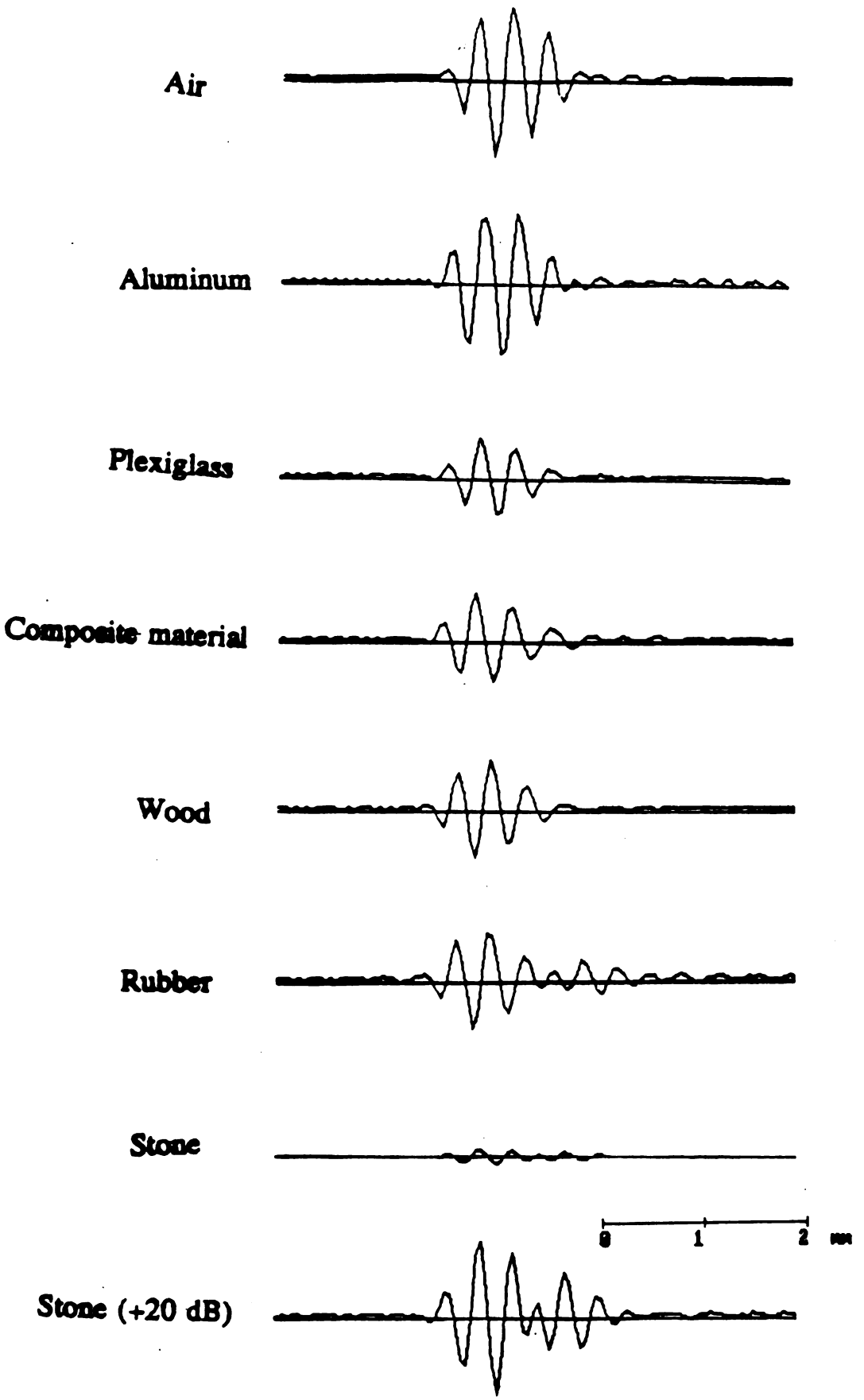

Figure 4.2.1 The waveforms of the reflected signals

explain why the power of two reflected signals detected at different time from water/air interface are slightly different.

Signal reflected from water/target interface

For a given input, the power of a reflected signal depends on the square of the reflection coefficient. The absolute values of reflection coefficients are given in Table 4.2.1.

From the published characteristics of materials, one can calculate the theoretical values of the reflection coefficients. For example, the density, the elasticity stiffness constant, and the viscosity of aluminum [3] are:

$$\rho_{al} = 2695\ kg/m^3$$
$$c_{al} \approx 11\times10^{10}\ N/m^2$$
$$\eta_{al} \approx 35\times10^{-5}\ N\cdot sec/m^2$$

From Eq. (4.2.9), the reflection coefficient is

$$R_{water/al} \approx \frac{(11.478-1)+j\omega\ 16\times10^{-15}}{(11.478+1)-j\omega\ 16\times10^{-15}} \approx 0.840$$

From the value of $R_{water/al}$ we can conclude that about 70.6 percent ($R^2_{water/al} \approx 0.840^2 \approx 0.706$) of the incident energy will be reflected from the water/aluminum interface.

Taking plexiglass as an example, the characteristics of which are

$$\rho_{pglass} = 1182\ kg/m^3$$
$$c_{pglass} \approx 8.5\times10^9\ N/m^2$$

The reflection coefficient is

$$R_{water/pglass} \approx \frac{(2.113-1)+j\,(\eta_{pglass}\omega)/(1.7\times10^{10})}{(2.113+1)-j\,(\eta_{pglass}\omega)/(1.7\times10^{10})}$$

If we assume the imaginary part is small, that is $\eta_{pglass} << (\frac{c_{pglass}}{\omega})^2$, we may approximate the reflection coefficient as

$$R_{water/pglass} \approx 0.358$$

Therefore, about 12.8 percent ($R^2_{water/pglass} \approx 0.358^2 \approx 0.128$) of the energy will be reflected from the water/plexiglass interface.

From the theoretical analysis, the ratio of the reflection coefficient is

$$\frac{R_{water/al}}{R_{water/pglass}} \approx \frac{0.840}{0.358} \approx 2.346$$

From the experimental results,

$$\frac{R_{water/al}}{R_{water/pglass}} \approx [\frac{Power_{water/al}}{Power_{water/pglass}}]^{1/2}$$
$$\approx [\frac{89956.47}{22289.42}]^{1/2} \approx 2.01$$

The experimental results are within 15 percent of the theoretical results.

4.2.2 The spectral difference between the reflected waveform and the incident waveform

The signals are transformed into the frequency domain by a FFT routine. Figure 4.2.2 is the spectrum of each signal detected. The spectral distribution of the reflected wave should be similar to that of the incident wave, when the reflection coefficient is real. Figure 4.2.3 is the spectral difference between reflected signal and incident signal. For comparison, the spectra have been normalized with respect to the incident power. From the spectral difference, one should be able to identify the nature of the target.

4.2.3 The sign of the reflection coefficient

From the power content of each reflected signal, one can evaluate the absolute values of the mean reflection coefficients. The sign of the reflection coefficient, however, can not be determined from such information. The sign of the reflection coefficient can be determined by correlation techniques. If the positive peak in the crosscorrelation of two signals is greater than the negative peak, the two signals must be in phase. Otherwise, they are out of phase. Since the reflection coefficient of the water/air interface is negative, we may determine the sign of reflection coefficient by correlating the echoes from the water/air reflection and the water/target reflection.

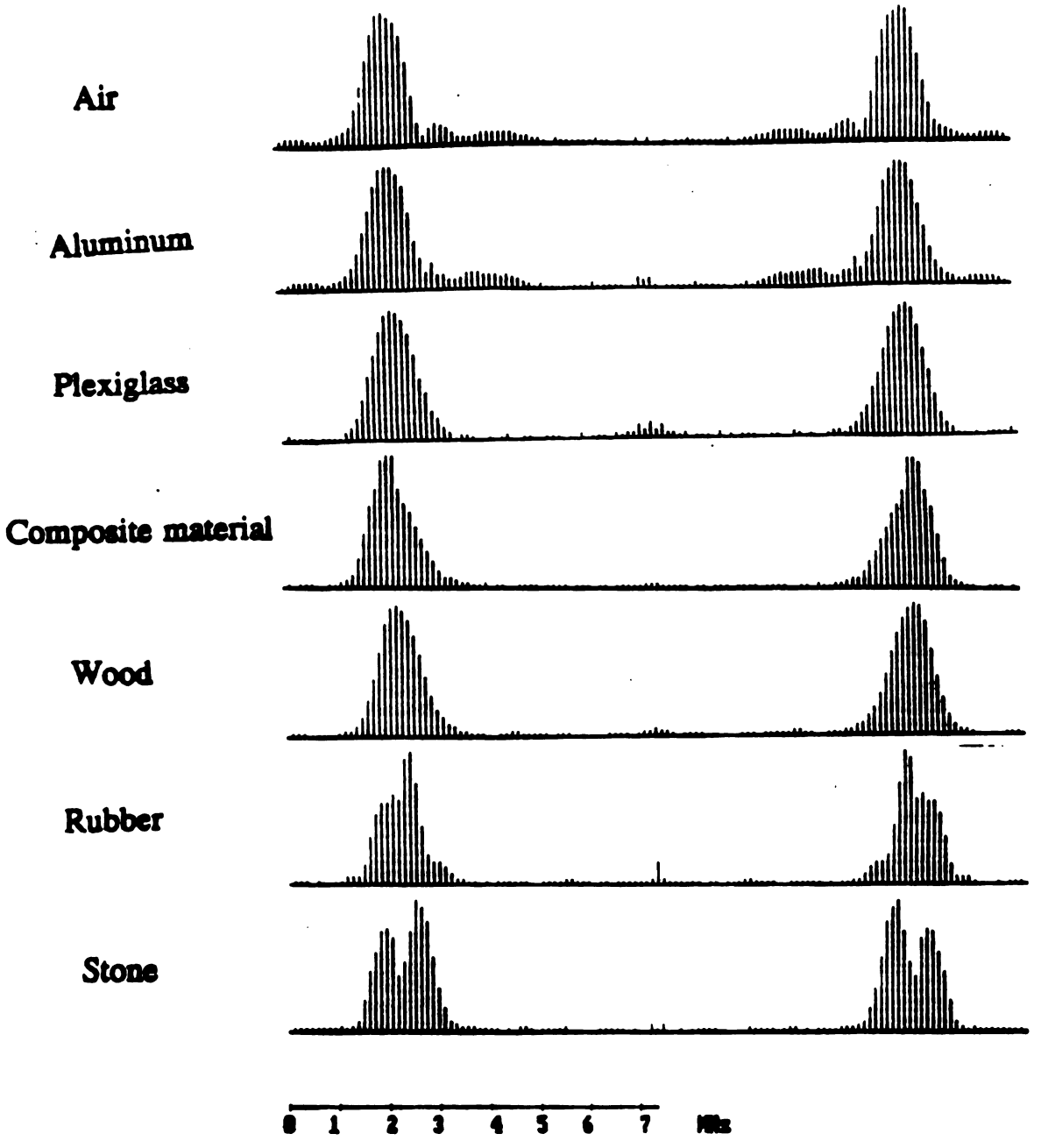

Figure 4.2.2 The spectra of the reflected signals

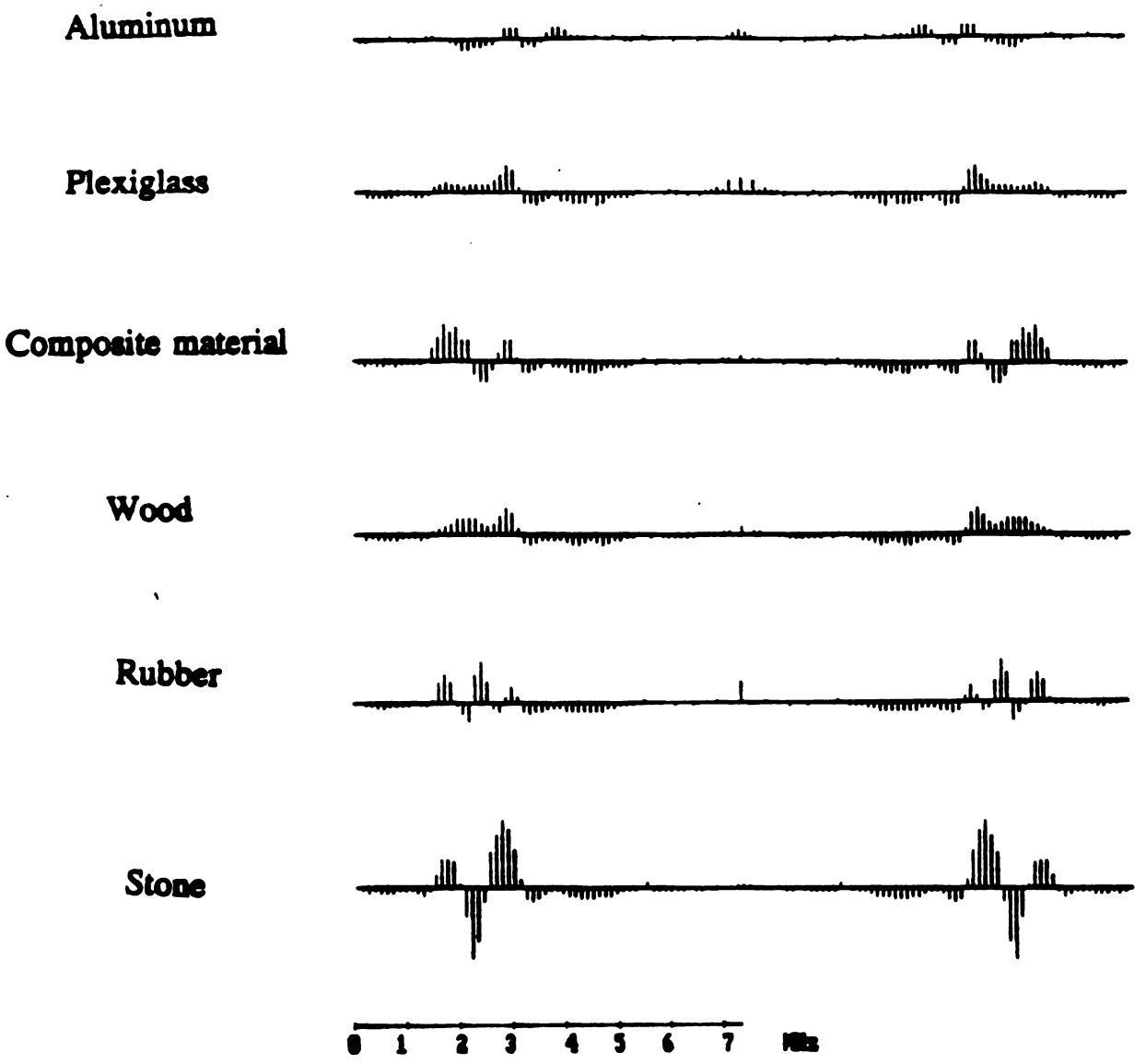

Figure 4.2.3 The spectral difference between the incidence and the reflection spectra

Table 4.2.2 The approximate reflection coefficients

Second medium	approximate reflection coefficient
Aluminum	+0.840
plexiglass	+0.208
composite material	+0.258
wood	-0.285
rubber	-0.317
stone	-0.008

Figures 4.2.4 - 4.2.11 show the correlation of each signal with the water/air reflection. From these figures, we find that the reflection coefficients of water/aluminum, water/plexiglass, and water/composite material are positive, while those of water/wood, water/rubber, and water/stone are negative. If we take $R_{water/al} = 0.840$ as the reference, we get the results shown in Table 4.2.2 for the approximate reflection coefficients for other materials.

The more accurate reflection coefficients can be obtained from the spectra of the incident and reflected signals at each frequency component, since the reflection coefficients at different operation frequencies are different.

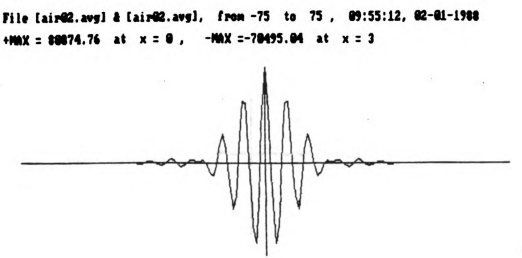

Figure 4.2.4 The autocorrelation of incident signal

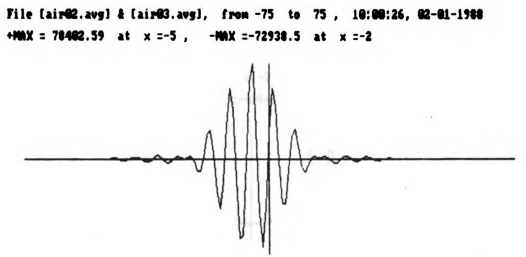

Figure 4.2.5 The crosscorrelation of incident waveform and waveform reflected from water/air interface

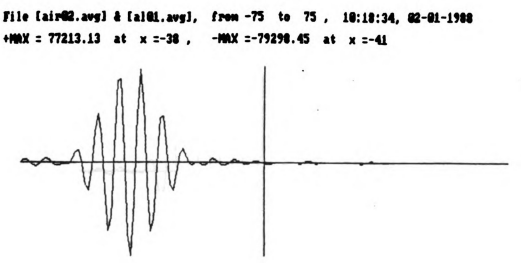

Figure 4.2.6 The crosscorrelation of incident waveform and waveform reflected from water/aluminum interface

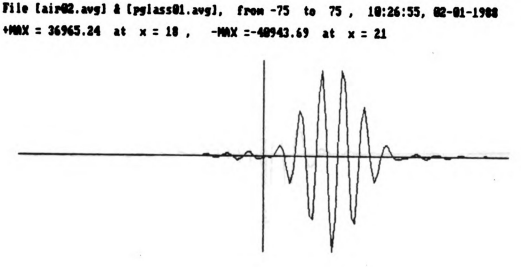

Figure 4.2.7 The crosscorrelation of incident waveform and waveform reflected from water/plexigalss interface

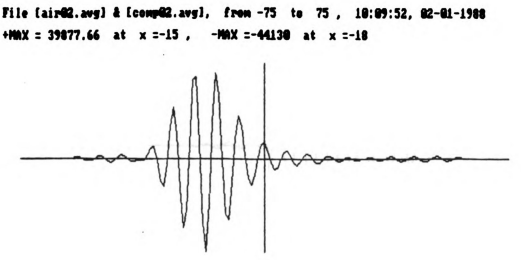

Figure 4.2.8 The crosscorrelation of incident waveform and waveform reflected from water/composite material interface

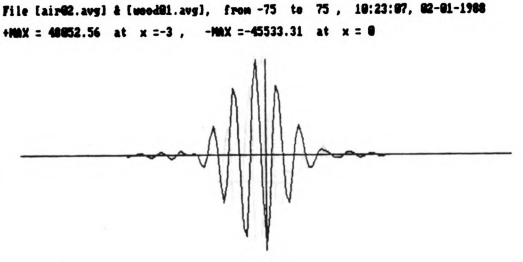

Figure 4.2.9 The crosscorrelation of incident waveform and waveform reflected from water/wood interface

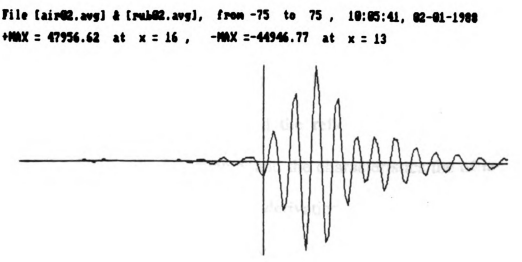

Figure 4.2.10 The crosscorrelation of incident waveform and waveform reflected from water/rubber interface

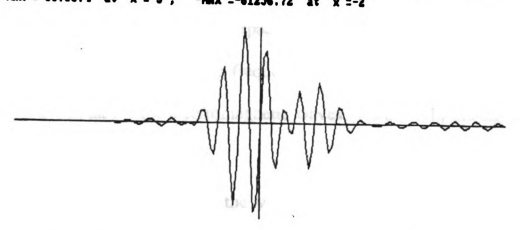

Figure 4.2.11 The crosscorrelation of incident waveform and waveform reflected from water/stone interface

4.3 Conclusion and Suggestion for Future Study

This thesis has derived the formulas for acoustic wave equations in terms of the attenuation constant α and the phase constant β in material media. The transmission coefficient and the reflection coefficient which turned out to be functions of frequency and the characteristics the of media were obtained. From the result of the derivation, the waveforms of the transmitted and the reflected signals depend not only on the characteristics of the medium, but also on the frequency components of the incident signal. With this in mind, it is possible to identify different media by their reflected video pulse shapes. The theory is verified by the expermental results.

Using the acoustic wave for remote sensing gives higher range resolution than using electromagnetic waves. The reason is that the wavelength of acoustic waves in a medium is five orders of magnitude shorter than that of the electromagnetic wave in free space. In addition to the shorter wavelength advantage, the operating frequencies for acoustic waves can be much lower than that for the electromagnetic waves. As a result, the signal is easier to record and process.

One essential requirement for the video pulse technique is that the reflected signal must be recored accurately, due to the fact that the shape of the reflected signal carries the media information. Therefore, a high sam-

pling rate analog-to-digital converter is needed. Once the signal is recorded, the data can be processed by software on a computer.

Experimentally, the approximate reflection coefficients can be determined by measuring the power ratio and evaluating the crosscorrelation of the reflected and the incident signals. The power ratio determine the mean magnitude and the peak of crosscorrelation determines the sign of the reflection coefficient. The precise reflection coefficients can be obtained from the spectra of the incident signal and of the reflected signal at each frequency component.

Although it is possible to obtain the medium density, the elasticity constant and the viscosity from the reflection coefficient, we did not obtain the experimental values in this thesis. In order to obtain these values, a much narrower video pulse must be used, so that a broader frequency spectrum can be sent to give a broader dispersive response from the media. By comparing the reflection coefficient at each frequency component, the characteristics of the materials can be determined.

Judging from the preliminary results of this work, we see that the video pulse technique has a high potential for application in many areas such as in cancer detection, nondestructive evaluation of materials, and remote sensing in land and sea environments. Before this technique can be applied in the

field, further theoretical as well as experimental must be carried out.

Bibliography

[1] Stewart, H. F., Stratmeyer, M. E., *An overview of Ultrasound: Theory, Measurement, Medical Application, and Biological Effects,* U.S. Department of Health and Human Services, July, 1982.

[2] Ronold W. P. King and Charles W. Harrison, Jr., *The transmission of electromagnetic waves and pulses into the earth* , J. of Applied Physics, Vol. 39, No. 9, Aug. 1968, pp.4444-4452.

[3] B. A. Auld, *Acoustic fields and waves in solids* , Vol. I, John Wiley & Sons, 1973, pp.1-190.

[4] Officer, *Introduction to the theory of sound transmission* , McGraw-Hill 1958, pp.1-83.

[5] Leenong Li, *Attenuation Measurement by Ultrasonic Techniques,* A Thesis for Master of Science, Department of Electrical Engineering and System Science, Michigan State University, 1987. pp. 17-60.

[6] Velimin M. Ristic *Principle of Acoustic Devices* , John Wiley & Sons, 1983, pp.1-51.

[7] Simon Ramo, John R. Whinnery and Theodore Van Duzer, *Fields and waves in communication electronics* , 2nd ed., John Willey & Sons, 1984.

[8] Robert T. Beyer and Stephen V. Letcher, *Physical Ultrasonics* , Academic Press, 1969.

[9] J. Szilard, *Ultrasonic Testing- non-conventional testing techniques* , John Willey & Sons, 1982.

[10] J. Blitz, M. Sc., and A. Inst. P., *Fundamentals of Ultrasonics* , Butterworths, 1963

[11] P. Filippi, *Theoretical Acoustics and Numerical Techniques* , CISM, 1983.